CHAPTER 5

5. SIMULATING PROTOTYPE MATERIALS BEHAVIOUR THROUGH FINITE ELEMENT MODELLING FOR WOLWEDANS DAM

5.1. BACKGROUND

In Chapter 4, instrumentation data for five prototype RCC dams was evaluated and a picture emerged that suggested that high-paste RCC in large dams demonstrates significantly less early shrinkage/creep during the hydration heating and cooling cycle than does conventional mass concrete (CVC) and than is assumed in traditional dam design.

Building on the largely qualitative evaluations in Chapter 4, Finite Element modelling is used in Chapter 5 to explore quantitatively the RCC materials behaviour that gives rise to the measured performance that differs from expectations.

On the basis of the earlier data evaluations, a number of questions persist as to the most realistic interpretation of certain of the apparent behaviour. This is particularly true in respect of residual stress and strain conditions in RCC between the open induced joints and the need was accordingly perceived to develop structural models to replicate the apparent RCC behaviour through analysis, isolating the actual characteristics by comparing measurements on a prototype with analytical predictions.

5.2. INTRODUCTION & DEFINITION OF OBJECTIVES

5.2.1. GENERAL

Chapter 5 presents four analyses; three addressing the early and operational performance of Wolwedans Dam and one addressing the early materials behaviour during construction at Changuinola 1 Dam

5.2.2. ANALYSIS 1: MODELLING INDUCED JOINT OPENINGS FOR WOLWEDANS DAM

In the review of the instrumentation data presented in Chapter 4, it became clear that a meaningful analysis of the low induced joint openings was not possible without an evaluation of the residual stress in between the open induced joints and an understanding of the impact on joint opening of the applicable hydrostatic water load.

The first analysis presented in this Chapter accordingly investigates the low measured induced joint openings at mid-dam height at Wolwedans through Finite Element modelling of the structure under load. Applying a parametric approach to focus in on the actual measured openings, an initial indication is developed of the behaviour of the constituent RCC, specifically in terms of the extent of shrinkage/creep that occurred during the hydration heating and cooling cycle.

The associated stress patterns on the induced joints and in the blocks in between are also reviewed.

5.2.3. ANALYSIS 2: SIMULATING TEMPERATURE DISTRIBUTIONS FOR WOLWEDANS DAM

In order to enable more accurate modelling, a study was required to establish the actual distribution of the temperature variations applicable across the surface and core zones of the Wolwedans Dam structure. For this purpose, measured temperatures and joint opening profiles from the instrumentation records were examined in detail.

5.2.4. ANALYSIS 3: MODELLING WOLWEDANS DAM PROTOTYPE BEHAVIOUR

A reduction in volume of the RCC in Wolwedans Dam due to shrinkage and creep during the hydration heating and cooling cycle will significantly influence the structural behaviour of the dam wall. By evaluating the measured crest displacements and joint openings against a number of shrinkage/creep scenarios, a good indication of the actual extent of the related effect is developed.

5.2.5. ANALYSIS 4: THERMAL ANALYSIS FOR CHANGUINOLA 1 DAM

The Thermal analysis for Changuinola 1 Dam was able to effectively predict surface gradient cracking that developed during June 2010 and the related modelling allowed some significant insights into the manner in which the RCC behaved during the early stages of the hydration heating and cooling cycle.

In order to illustrate the related findings, a brief description of the Thermal study for Changuinola 1 Dam is included in this Chapter.

5.3. ANALYSIS 1: MODELLING INDUCED JOINT OPENINGS

5.3.1. ANALYSIS APPROACH & PROTOTYPE BEHAVIOUR TO BE MODELLED

5.3.1.1. General

As discussed in Chapter 4, comparing the early temperature-time history at Wolwedans Dam[1, 2, 3, 4 & 5] with the concurrent induced joint displacements indicated that the joints started opening essentially once the internal RCC temperature dropped below the original placement temperature, suggesting that no shrinkage, or creep, or anything other than linear-elastic behaviour, had occurred in the green RCC during the process of concrete hydration[2]. This behaviour is reflected on **Figures 5.1** and **5.2**, which illustrate typical temperature and joint opening histories for the first five years of the life of the dam, for the internal zone of the structure.

Focusing on the third level of instrumentation, installed across 16 joints at approximately mid dam height (RL 66.250 m), the primary purpose of the investigations presented in this Chapter was to gain an understanding of the low measured induced joint openings by modelling the RCC behaviour within the body of the dam structure. By replicating similar joint openings on the model as measured on the prototype, under the same load conditions, it was considered possible to develop a picture of the thermal and structural behaviour of the dam wall and, by implication, to evaluate the performance of RCC as a material under these conditions.

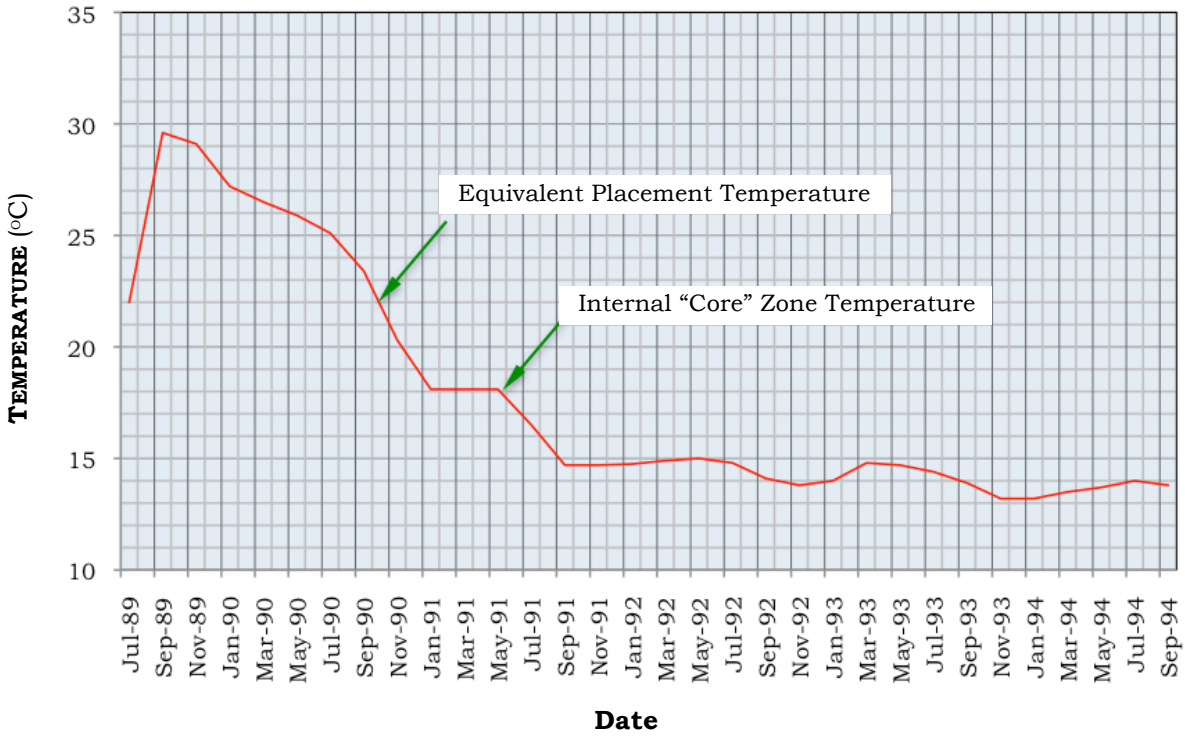

Figure 5.1: Temperature-Time History for Wolwedans Dam[2]

At elevation RL 66.250 m, the central blocks of the dam are sufficiently high to be largely free of the influence of any foundation restraint, but the RCC section is still adequately thick to ensure that the centre is well insulated from surface temperature variations. The dam wall is divided into seventeen blocks by sixteen induced joints at this level, with the joints numbered from 7 to 22 from the left to the right bank (**Figure 5.3** & **Figure 2.13**). Only three of the induced joints at Wolwedans actually opened to any real extent[2], specifically Joint Nos. 8, 14 and 17, and while the instrumentation records under scrutiny in this study cover a period of approximately 5 years, it is important to take cogniscance of the fact that full hydrostatic loading was essentially continually present from 2 years after construction completion.

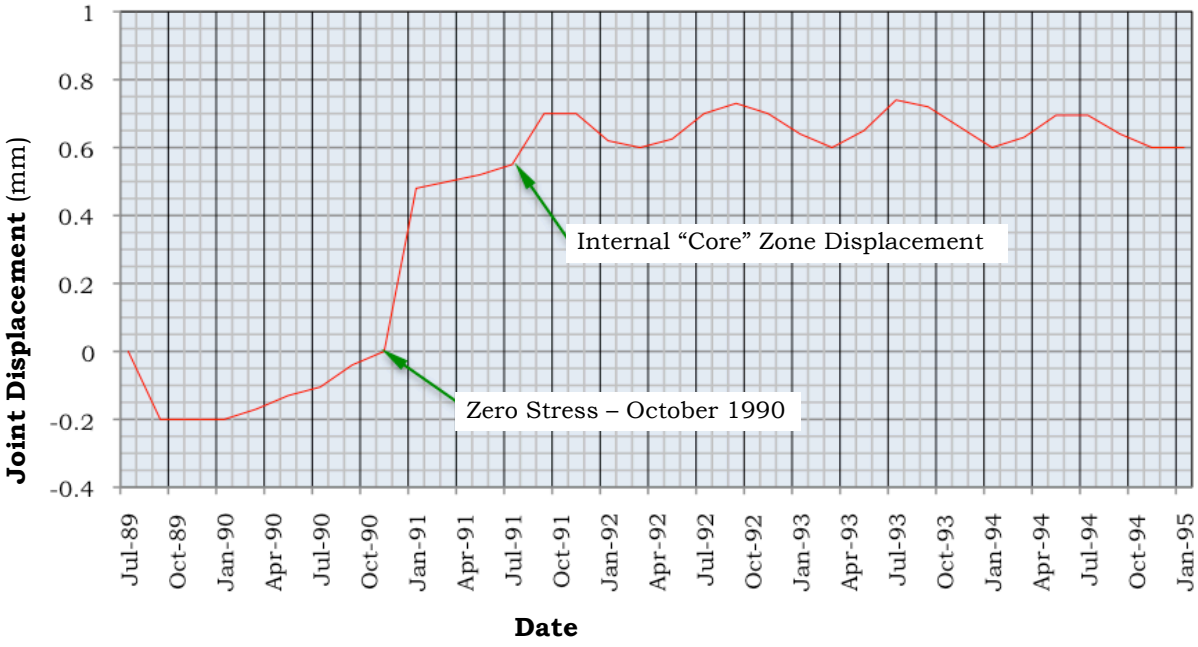

Figure 5.2: Joint Displacement – Time History for Wolwedans Dam[2]

5.3.1.2. Apparent Measured Behaviour

All of the induced joints at Wolwedans were comprehensively instrumented[4], with four levels of instruments and a minimum of 2 long-base-strain-gauge-temperature-meters (LBSGTMs) across each joint at each level. Despite all joints being weakened through de-bonding 25% of the RCC contact area, only three of the 16 joints at elevation RL 66.25 m demonstrated any real opening. In view of the fact that the dam structure took a period of approximately 3 years to cool to an equilibrium temperature cycle, the impoundment was essentially full by the time the first cold internal winter temperatures were experienced. Accordingly, no instrumentation data at a representative low temperature is available for an empty dam and the displacement information on the joints correspondingly represents the structural performance under temperature drop and hydrostatic loading.

At either end of the structure at elevation RL 66.25 m, the dam wall is obviously in contact with the foundation and accordingly experiences restraint. While the total length on the centerline of the wall at this elevation measures approximately 150 m, the distance between the outermost joints is 137 m and it is considered that this distance effectively represents the length of the wall over which shrinkage as a consequence of temperature drop can occur.

By winter 1993, the hydration heat had essentially dissipated from the core of the dam structure and the minimum temperature within the dam wall at elevation RL 66.25 m was measured as approximately 14°C. Comparing this figure with an RCC placement temperature that averaged approximately 22 – 22.5°C accordingly implied a maximum apparent core temperature drop of approximately 8 to 8.5°C, which can be compared with a total summed associated simultaneous measured joint opening, on the centreline of the dam wall, of 3.4 mm. While this full joint opening was concentrated at just 3 induced joints (Nos. 8, 14 and 17), surface joint opening was also experienced at a further four induced joints (Nos. 11, 12, 18 and 21), where maximum displacements of approximately 0.5 mm were observed. Surface temperature and joint opening variations are subsequently explored under section 5.4.

The above figures relate to the winter of 1993, before the induced joints were grouted. They are, however, similarly applicable for August 1995, after grouting, when an equivalent temperature drop and comparable joint openings were measured at RL 66.25 m.

Over a total length of approximately 137 m, the summed contraction on the joints can be translated into a direct tensile strain of 25 microstrain. For an 8°C temperature drop, such a strain would suggest an associated thermal expansivity of approximately 3×10^{-6}/°C, which is significantly less than half of the figure that would be anticipated for a concrete comprising quartzitic aggregates.

As mentioned in Chapter 4, it is considered that the apparent discrepancy in thermal expansivity/induced joint opening could relate to underestimated residual tensions within the uncracked RCC, a lower actual effective structural temperature drop, an actual lower thermal expansivity, creep of the RCC in tension, or a combination these factors. The imposition of the hydrostatic water load will obviously also significantly influence the displacements across the joints that have opened as a consequence of thermal shrinkage. In view of the repetition of the same joint openings at RL 66.25 m two years later, it can be concluded that joint grouting was not the cause of the smaller than expected joint openings. The primary purpose of the analyses addressed in this Chapter was accordingly to simulate the displacements measured on the prototype structure and consequently to identify the origin of this apparent discrepancy, thereby gaining an understanding of the associated behaviour of RCC under early thermal loads.

5.3.2. 3-DIMENSIONAL ANALYSIS OF WOLWEDANS DAM

5.3.2.1. Wolwedans Dam

Wolwedans Dam was used as the central focus for the analyses completed as a consequence of the availability of comprehensive instrumentation records[1, 3, 4, 5, 6 & 7], full geometrical details and its familiarity to the author. Wolwedans is a single curvature arch/gravity dam with a maximum height of 70 m, an extrados arch circular radius of 135 m and a crest length of 270 m. The dam and its instrumentation are described in more detail in Chapter 2. A total number of 27 induced joints were comprehensively instrumented at Wolwedans Dam, for the primary purpose of establishing the degree to which each joint opened and the associated need for grouting to re-establish the structural continuity of the arch as a consequence of post-hydration thermal shrinkage.

The dam was completed and began impounding water early in 1990[1], filling to capacity and spilling for the first time in October 1992. A programme of joint grouting was carried out during late winter 1993.

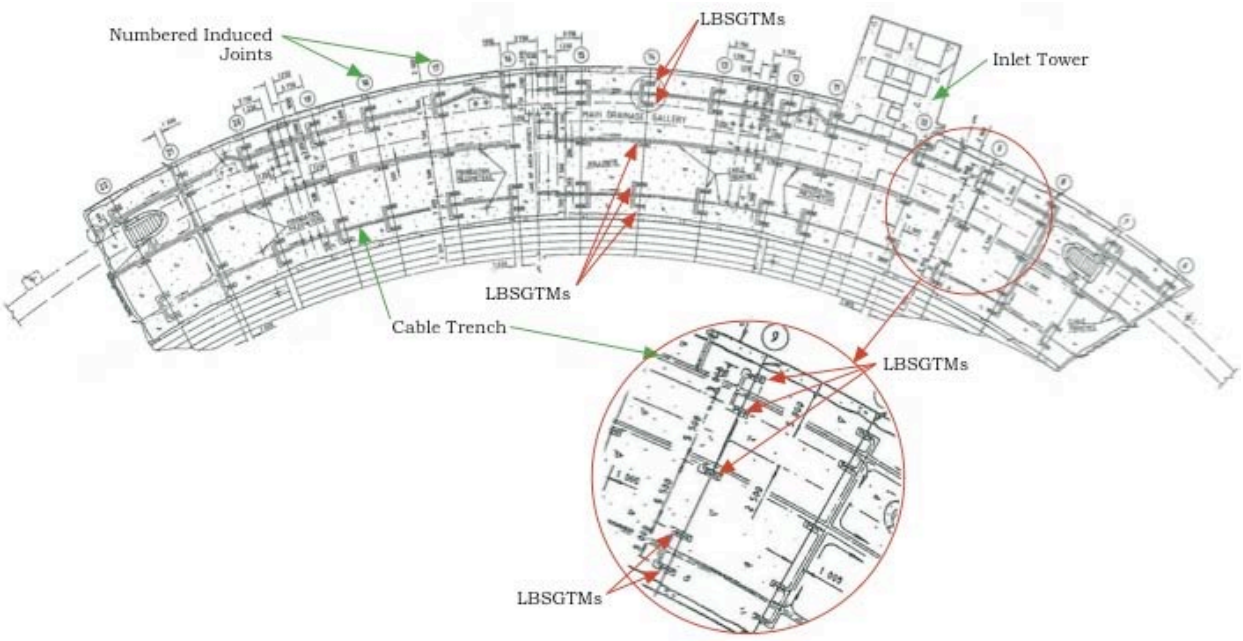

Figure 5.3: Wolwedans Dam – Illustration of Instrumentation at RL 66.25 m[1]
(For more detail see **Figure C3**)

5.3.2.2. FE Analysis Model

For the purposes of the early investigative analyses addressed in this Chapter, a comprehensive, 3 dimensional Finite Element model was established using the COSMOS[8] general structural analysis software. The model simulates the dam and the foundation, with each radial dam block between induced joints being developed as separate parts and joined with Gap elements. Ten-noded solid tetrahedral elements

were used in a high-density mesh. For analyses in which induced joints were not allowed to open, replicating the fact that these joints had not opened on the prototype, the Gap elements were simply omitted. Representations of the FE model are presented for illustration on **Figures 5.4** and **5.5** overleaf.

In accordance with accepted practice for a rockmass with a similar deformation modulus to that of the dam concrete[9], the modelled foundation block extended approximately 1.5 x dam height (H) below, upstream and downstream of the dam and 1 x H on either flank. At the extremes, the foundation block was fully restrained.

Although it is not strictly representative of the actual situation applicable on the prototype structure, temperature drops were applied for the preliminary analyses as a single drop from a reference temperature (zero stress temperature) to all areas of the dam wall, but not the foundation. In reality, the internal and external zones of the dam wall will be subject to different effective structural temperature drops, while heat will move into the cooler foundation from the warm dam, and the foundation will provide additional insulation to the adjacent concrete during seasonal cycles.

An evaluation of the actual distribution of temperature drops is presented as a later part of this Chapter. For the purpose of the early investigations addressed here, however, a simplified approach was considered appropriate.

5.3.2.3. Materials Properties

While a number of the RCC materials properties for Wolwedans Dam are known[1], it was necessary to make a number of assumptions for the analyses undertaken. The following properties were available from site and construction records[1]:

Average RCC Density:	2400 kg/m^3
Average 1 year RCC compressive strength:	35 MPa

The following materials property assumptions were made for the analyses completed:

RCC Elastic Modulus:	15 - 25GPa
RCC Poisson's Ratio:	0.20
Rockmass/Foundation Elastic Modulus:	8 - 15GPa
Rockmass/Foundation Poisson's Ratio:	0.30

In view of the fact that no measured data is available for the thermal expansivity of the RCC at Wolwedans, but on the basis of knowledge of the quartzitic constituent aggregates, it was assumed that an applicable value would lie between 9 and 11 x 10^{-6}/°C[10]. Within typically realistic ranges for concrete and rock[11], the Poisson's ratio has very little influence on the behaviour of interest and accordingly, typical values were assumed, with no variations.

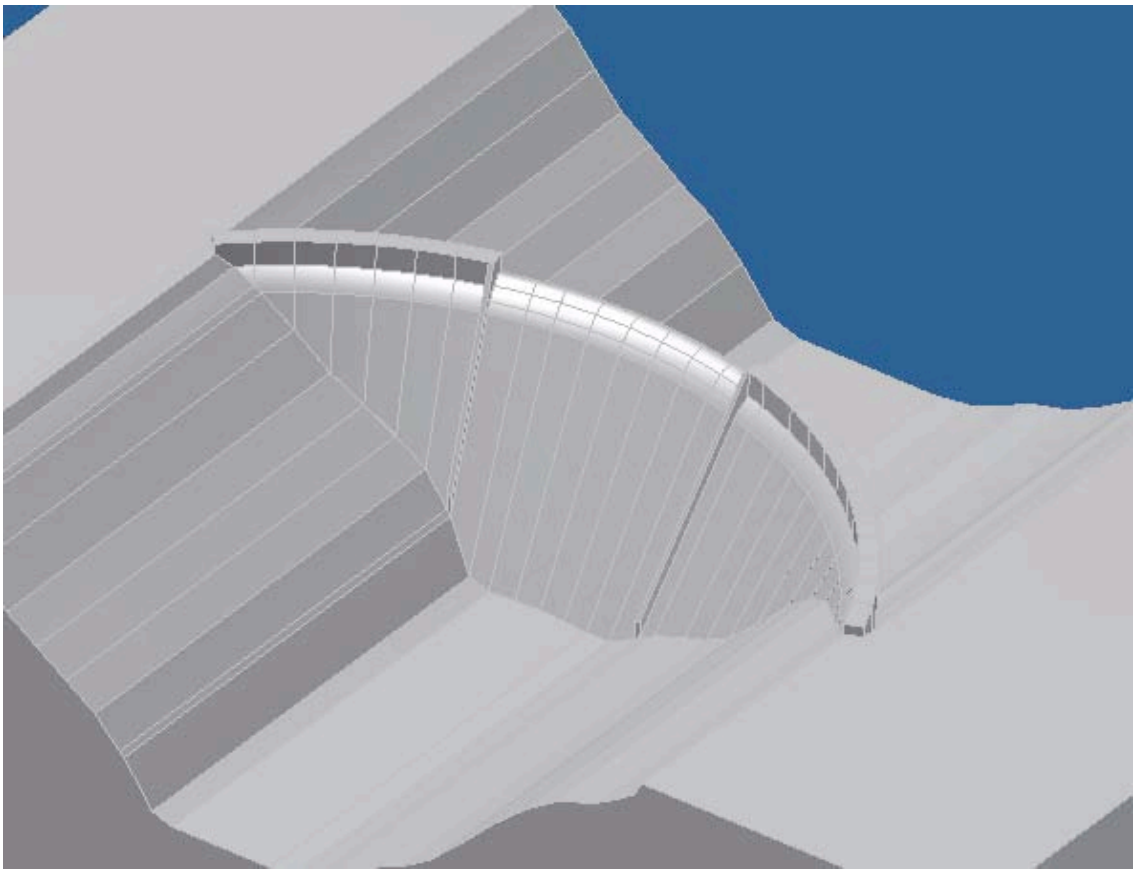

Figure 5.4: Wolwedans Dam FE Model – Illustrating "Part" Structures

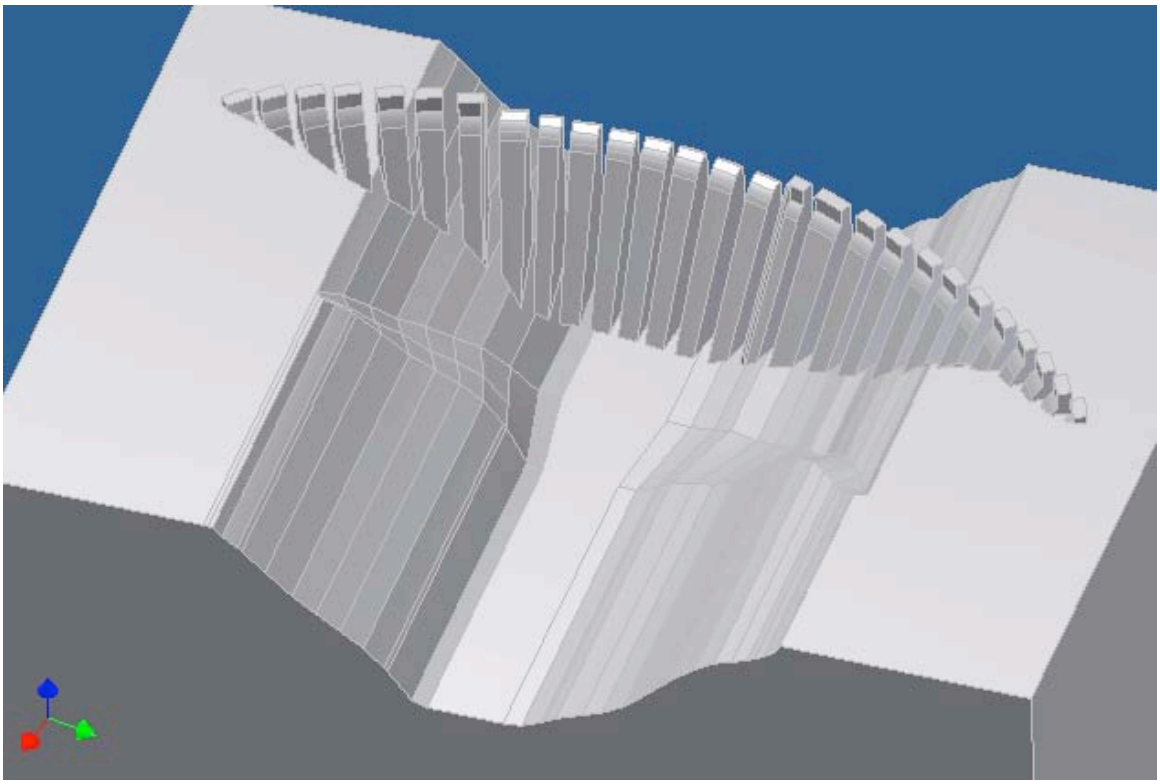

Figure 5.5: FE Model –Split & Lifted to Illustrate Location of "Gap" Elements

5.3.2.4. Analysis Development

A series of analyses was completed in the process of developing a first representation of the actual prototype behaviour characteristics. Initially, a uniform 8°C temperature drop was applied across the full dam, with no hydrostatic, gravity or uplift loading. A thermal expansivity of 10 x 10^{-6}/°C was assumed, together with a long-term deformation modulus of 15 GPa and the early analyses were linear-elastic, allowing all induced joints to open. The sustained E modulus applied is reduced from the instantaneous, tested value to take cognisance of the inelastic behaviour of concrete that is manifested as a reversible creep under sustained loading.

Subsequently, the input and materials parameters were varied, while only joint Nos 8, 14 and 17 were allowed to open, in accordance with the prototype. The following step involved the addition of hydrostatic, uplift and gravity loadings to simulate as realistically as possible the actual conditions under which the prototype joint measurements were taken.

For each analysis, the opening of each induced joint was evaluated at elevation RL 66.25 m, on a local co-ordinate system, on the centreline of the dam, as illustrated on **Figure 5.6**. In addition, the level of residual stress in a direction parallel to the dam axis was reviewed in the centre of the blocks between open induced joints and in the flank zones of the structure, where no joint openings were observed.

Early analyses demonstrated potential variations of the E modulus of the rockmass/foundation to have only a minor influence on the magnitude of the induced joint openings. In view of the fact that it would never be possible to develop any degree of certainty in respect of the foundation rockmass properties, a more conservative stiffer foundation was assumed for all subsequent analyses, with an E modulus of 15 GPa.

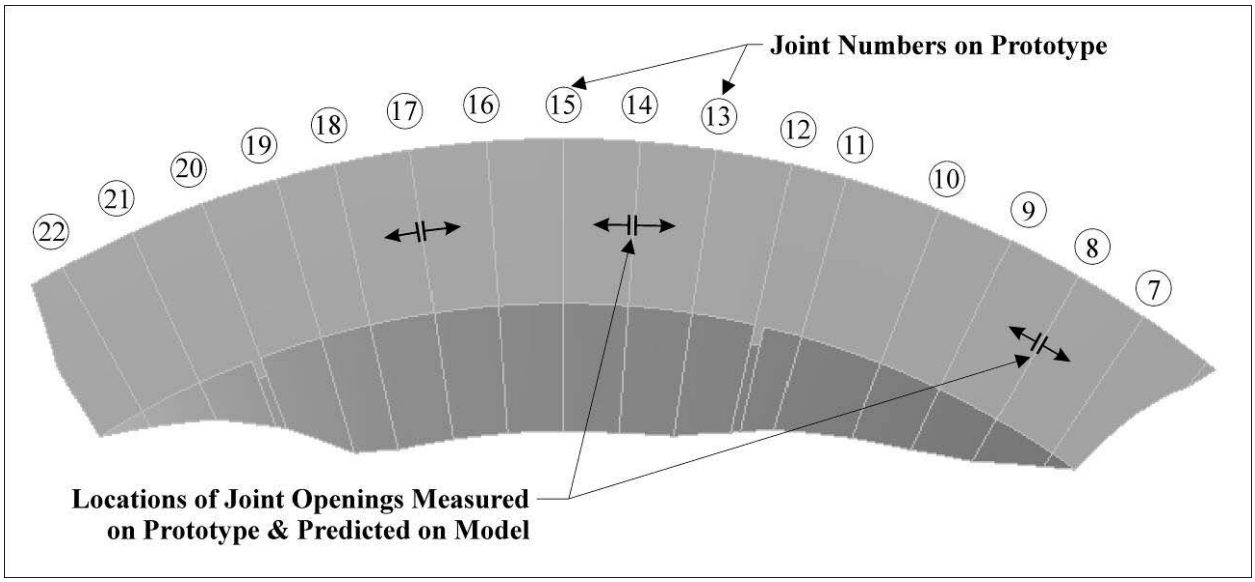

Figure 5.6: Horizontal Section through FE Model Illustrating Location of Joint Opening Reference Points

5.3.2.5. Analysis Findings

Initial Indications

The early analyses quickly demonstrated that the site topography, the steep abutments and the arch geometry exert significant influence on the displacements across the open induced joints. However, for the analyses without gravity, or hydrostatic water loading and all joints allowed to open, a very direct correlation between joint opening and predicted thermal shrinkage was evident, suggesting very low levels of residual stress within the RCC blocks, whether every induced joint, or only every third joint, was allowed to open.

For an 8°C temperature drop and a thermal expansivity of 10 x 10^{-6}/°C, the summed total of all horizontal joint openings, with all joints allowed to open, was indicated as 10.8 mm, while the indicated residual stresses between induced joints was negligible.

For a similar analysis, with only joint Nos. 8, 14 and 17 allowed to open, the summed horizontal joint openings was indicated as 10.5 mm, while residual stresses between induced joints were typically less than 50 kPa on the blocks between induced joints and less than 100 kPa on the blocks at either end of the dam structure. Converting the average residual stress between open joints on the basis of a deformation modulus of 15 GPa confirms that a total strain shrinkage of approximately 0.3 mm is retained in residual stress.

For an applicable dam wall length of 137 m, an 8°C temperature drop and a thermal expansivity of 10 x 10^{-6}/°C should produce a total joint opening of 11.0 mm, if no residual tension remains, confirming the accuracy and representivity of the analyses completed.

Adding, gravity, hydrostatic and uplift loading in the case of this last analysis, with joint Nos. 8, 14 and 17 allowed to open, the summed horizontal joint openings reduced to approximately 3.5 mm.

Modelling to Reproduce the Prototype Measurements

In modelling a dam structure using Finite Elements, a specific problem relates to the imposition of gravity as a load case. When gravity is imposed as a load on the completed dam, but not the foundation, the dam structure will want to pull downwards into the valley bottom. This tends to develop shear forces between the shoulders/abutments of the dam structure and its foundation on the FE model (see **Figure 5.7**). When specific discontinuities are present, or when the abutments flatten with height, a hanging effect is created and tensions are developed in the dam structure model, which would not be so pronounced in reality, where gravitational forces are progressively developed during the construction process. Reviewing the structural modelling for Wolwedans Dam, such an effect is evident at Joint No. 8, particularly when this joint is allowed to open. Ignoring the hydrostatic loads, a joint opening of 3.57 mm is anticipated by the model, 2.85 mm associated with a temperature drop of 8°C and 0.72 mm associated with the imposition of gravitational

forces. Such an effect is not present at Joint Nos. 14 and 17, where the impacts of foundation anomalies and gravity-related shears are reduced due to height above foundation and location close to the centre of the dam. In order to make a more realistic comparison of the model joint openings with those measured on the prototype, the unrealistic modelling effects caused by the imposition of gravity as a load were taken into account by subtracting 0.72 mm from the opening on Joint No. 8 at RL 66.25 m for all subsequent analyses.

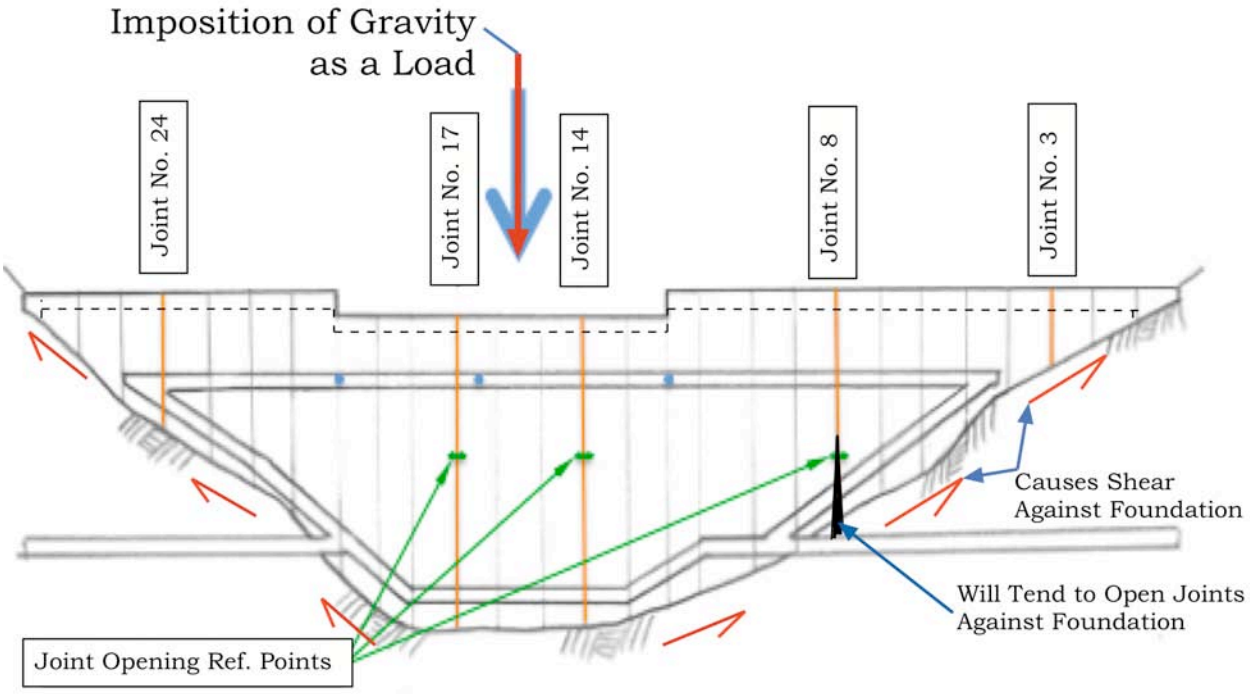

Figure 5.7: Illustration of Impact of Imposing Gravity as a Load

To simulate the prototype structure loading, gravity, hydrostatic and uplift loads were added to the FE analyses and only joint Nos. 8, 14 and 17 were allowed to open, as only these had opened on the prototype. In order to isolate the observed prototype behaviour, a number of the model input parameters and properties were varied as follows (with the remainder fixed as indicated under 5.3.3):

Property/Input Parameter	Unit	Values Considered
Temperature drop	˚C	8, 8.2, 8.5 & 8.7
Thermal expansivity	Microstrain / ˚C	9, 10, 10.5 & 11
RCC Elastic Modulus	GPa	15, 20 & 25
Uplift	-	As per design & 50% design

The hydrostatic load was input with the impounded water surface at FSL, while uplift was modelled as two load cases; firstly as full hydrostatic at the upstream face, reducing by 2/3 on the line of the gallery and to zero at the toe (as per the dam design - no tailwater applicable) and secondly as 50% of the same load (50% of dam design load). While the former uplift loading represents a typical design assumption, the latter is probably more realistic for a competent, grouted and drained foundation.

The joint openings on the centreline of each of the joints allowed to open was subsequently summed and compared with the total joint displacements measured on the prototype.

5.3.2.6. Modelling Results

Table 5.1 provides a summary of the study results.

Table 5.1: Joint Openings at RL 66.25 m for Various Scenarios

Scenario						Joint Openings			
Scenario	**Uplift**	**E Modulus Dam**	**E Modulus Foundation**	**Thermal Expansion Coefficient**	**Temperature Drop**	Jt. 8	Jt. 14	Jt. 17	Combined
No.	% Design	(GPa)	(GPa)	(x 10^{-6}/°C)	(°C)	(mm)	(mm)	(mm)	(mm)
1	50	15	15	10	8	1.40	0.52	0.85	2.77
2	50	20	15	10	8	1.56	0.77	1.17	3.50
3	50	25	15	10	8	1.72	0.88	1.37	3.97
4	50	15	15	11	8	1.75	0.76	1.12	3.63
5	50	20	15	11	8	1.97	0.93	1.47	4.37
6	50	25	15	11	8	2.09	1.06	1.71	4.86
7	50	15	15	9	8	1.01	0.38	0.61	2.00
8	50	20	15	9	8	1.22	0.56	0.87	2.65
9	50	25	15	9	8	1.36	0.65	1.07	3.08
10	50	15	15	10	9	1.84	0.81	1.20	3.85
11	50	20	15	10	9	2.04	1.01	1.55	4.60
12	50	25	15	10	9	2.16	1.13	1.79	5.08
13	100	15	15	10	8	1.36	0.55	0.81	2.71
14	100	20	15	10	8	1.56	0.74	1.10	3.41
15	100	25	15	10	8	1.70	0.83	1.33	3.86
16	100	20	15	10	9	2.03	0.96	1.50	4.49
17	100	25	15	10	9	2.15	1.09	1.73	4.97

5.3.2.7. Discussion

When initially running the above analyses, it was assumed that it would be necessary to review the joint openings against a preliminary "no creep" case and subsequently to increase the Temperature drop to account for shrinkage/creep. This, however, did not prove realistically possible, as the variation of the result data, around credible RCC input parameters, did not seem to allow for such an eventuality. The only scenario to approach the measured joint openings that might have possibly allowed any creep would indicate 50% design uplift, a coefficient of thermal expansion of 10 x 10^{-6}/°C, a temperature drop of 9°C and an E modulus of 15 GPa for the dam. However, the indicated joint openings were slightly larger than those measured, while any creep that might have occurred would relate to the difference in temperature drop between 9 and 8°C, which is realistically within the margin of error of the analysis. The analyses, however, indicated higher crest displacements than actually measured for this scenario.

In reviewing the results in **Table 5.1**, it is important to include a number of significant considerations. The assumptions for uplift in dam design (see **Appendix B**) are conservative and in the case of Wolwedans, the abutments are drained by tunnels and the foundation pore pressure measurements have never indicated any significant pressures[7]. Accordingly, 50% design uplift load is considered the more realistic loading situation. For a concrete manufactured using a quartzitic aggregate in South Africa, a high coefficient of thermal expansion would usually be expected[10] and accordingly, it is considered that any associated value below 10 x 10^{-6}/°C would not indicate a high credibility.

Consequently, in terms of reproducing the prototype behaviour, the most credible scenarios modelled would be either No. 2, or No. 4. While the individual displacements predicted for each of the joints are anyway more accurate in the case of Scenario 2, the analyses indicated excessive crest displacements for Scenario 4.

As can be seen from **Table 5.1**, the typical, summed joint openings for the properties and loads considered varied between 2 and 5 mm. Changing the uplift load by 50% indicated an impact of less than 3%, with increased uplift causing increased joint closure, while higher temperature drops and coefficients of thermal expansion unsurprisingly resulted in increased joint openings. Closure of the induced joints under load was demonstrated to reduce with increasing RCC E modulus.

While it is not considered that the preliminary modelling undertaken could identify a single solution, or behaviour mode, with any certainty, on the basis of indicating the closest individual and combined joint openings to those measured on the prototype structure, Scenario 2 is considered most representative of the reality. Accordingly, the most representative behaviour of Wolwedans Dam in July 1993 was represented by an 8°C temperature drop, an RCC coefficient of thermal expansion of 10 x 10^{-6}/°C, an RCC elastic modulus of 20 GPa, a foundation elastic modulus of 15 GPa and 50% uplift load. In view of the fact that an actual temperature drop from placement of approximately 8°C was measured, this scenario would suggest that no significant

shrinkage or creep had in fact occurred at Wolwedans Dam during the hydration heating and cooling cycle.

In the case of Scenario 2, the maximum residual tensile stress between the internal joints was indicated to lie between 23 and 26 kPa, while the maximum residual tensile stress between the abutments and the external induced joints was indicated as between 220 and 290 kPa.

Table 5.2 compares the actual and predicted openings on the centre of each of the "open" induced joints for Scenario 2.

Table 5.2: Predicted and Measured Displacement on Induced Joints for Full Dam, 8°C Temp. Drop, 10 x 10^{-6}/°C Thermal Expansivity, 20 GPa RCC Modulus, 50% Design Uplift & 15 GPa Foundation Modulus.

Joint No.	Displacement on Centre of Joint (mm)	
	Measured on Prototype	Predicted on FE Model
8	1.0	1.56*
14	0.95	0.77
17	1.45	1.17
Total	**3.4**	**3.50**

* - Joint displacement with unrealistic gravity-modelling related displacement deducted (2.28 – 0.72), as discussed under 5.3.3.3.

5.3.2.8. Residual Stress Levels

The low levels of the residual stress indicated between the induced joints through the analyses completed clearly demonstrate the cause of only three induced joints opening to any depth at Wolwedans Dam. Even with the weakening created by de-bonding surfaces on the joints, tensile stresses of less than 300 kPa are not likely to induce cracking. With residual stress levels as low as 22 kPa between the open joints, it is clear that a joint spacing at Wolwedans Dam of approximately 30 m would have been quite adequate. Despite surface and internal de-bonding being provided on 16 joints at RL 66.25 m, joint opening even at the surface was only measured on 7 joints.

5.3.3. DISCUSSION & CONCLUSIONS

5.3.3.1. Validity of Modelling

Despite the simplicity of the modelling completed, the lack of accuracy in respect of the distribution of the temperature drop loading applied and the linear materials properties assumed, a meaningful simulation of the prototype dam behaviour was developed. Admittedly, the analyses focused only on joint openings on the centreline of the dam wall and at an elevation where foundation restraint does not play a significant role, but the reproduction of the prototype behaviour with temperature

drops that can be substantiated through measurement and materials properties in line with expectations confirms the validity of the apparent findings.

The structural function of an arch/gravity dam under hydrostatic and temperature drop load is such that displacements throughout the dam wall will be dependent on the placement temperature conditions within the upper section of the dam wall, where structural contact occurs first. This is illustrated on **Figure 5.8**, which demonstrates that sufficient arch action is incurred within the top 20 m of the dam structure to carry the applied water load. If the effective placement temperature within this specific zone were to be different, the structural action of load transfer within the wall would change significantly. In view of the fact that the applicable temperature drop within the top section of the dam structure, where seasonal temperature variations will be greater, is likely to be different to the lower section, careful thermal analysis will be required to ensure a realistic temperature drop assessment in this zone.

In the case of an analysis of this nature, it is not considered possible to predict strains and displacements with complete accuracy, as other, unmeasured factors could influence the performance of the prototype; such as variations in foundation stiffness, differential surface heating caused by solar radiation, variable placement temperatures at different heights and locations on the dam wall, etc. In the case of Wolwedans Dam, additional influences will include the fact that the first three blocks of the dam wall were constructed using a conventional formed joint at Joint No. 3 and the fact that the dam was constructed in two separate seasons, allowing substantial cooling of the lowest 15 m of the dam, which caused cracks to open at Joint Nos. 11, 14, 16 and 17, before placement was re-started for the remaining 55 m of the dam.

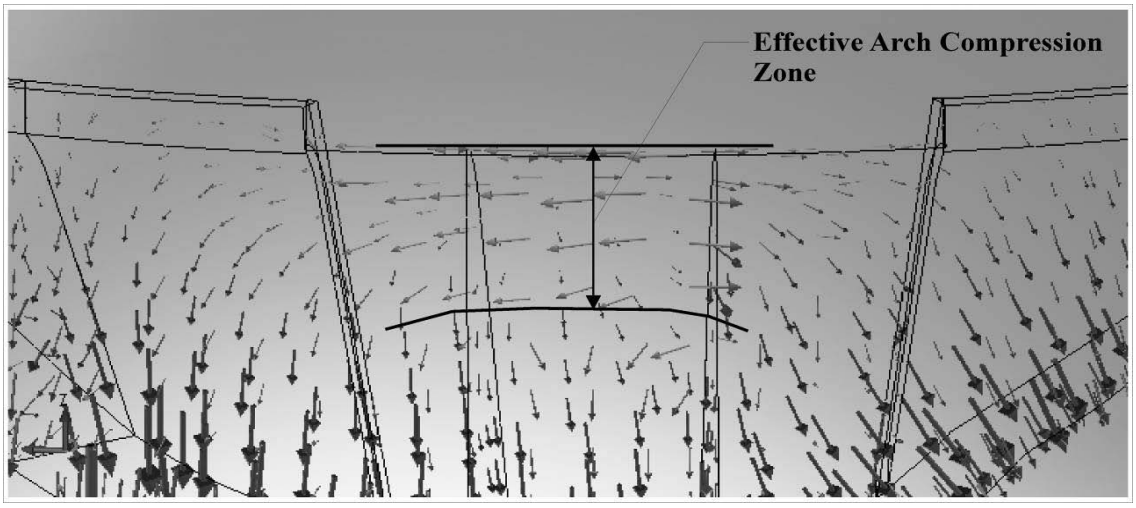

Figure 5.8: Arch Stress Distribution for FSL + 8ºC Temperature Drop

Furthermore, the effective temperature drop experienced across the full structure was undoubtedly not constant. However, considering all of these potential difficulties in simulating the actual conditions, the modelled joint openings are in fact surprisingly consistent with the measurements from the prototype.

While the applied RCC deformation modulus of 20 GPa is relatively high, testing on RCC cores revealed an average modulus at 24 months age of approximately 32 GPa, indicating that the modulus applied for analysis concurs well with an anticipated sustained deformation modulus equivalent to 60 to 70% of the instantaneous value[11].

The next step in the development of the investigation of the early thermal behaviour of RCC will accordingly encompass detailed thermal analysis to establish a more realistic temperature drop distribution and to enable a comparison of the profile of the induced joint openings across the width and height of the dam wall.

5.3.3.2. Summary of Findings

The preliminary analyses presented indicate that the apparent discrepancy between the predicted and apparent openings on the induced joints at Wolwedans Dam can be directly ascribed to the application of the hydrostatic, uplift and gravity loads.

Furthermore, the analyses clearly demonstrate that a simple, linear elastic RCC materials model can be applied to relatively accurately replicate the apparent thermal and structural behaviour of a prototype RCC structure.

The analyses consequently confirm the indications that the applicable long term-temperature drop load is significantly closer to the difference between the placement temperature and the final cold winter cycle temperature within the dam wall than the difference between the maximum hydration temperature and the cold winter cycle temperature, as more generally applied as part of accepted practice for CVC[12] and RCC dams. The modelling completed accordingly endorses the observations made through instrumentation on the Wolwedans, Knellpoort and Çine Dams.

5.3.3.3. Value of Findings

The findings of these preliminary analyses provide a definitive indication that the early behaviour of RCC in dams under thermal loading is different to that of CVC and although more detailed and substantiated investigation is still necessary, the outcome of the work presented in this Chapter provides a platform and a validation for developing more detailed studies. Furthermore, it is considered that the cross correlation of confirmatory evidence from three prototype structures, and the simplicity with which the prototype behaviour was replicated through modelling, together already serve to provide confidence in the analysis results.

5.4. ANALYSIS 2: SIMULATING TEMPERATURE DISTRIBUTIONS FOR WOLWEDANS DAM

5.4.1. BACKGROUND

The initial structural modelling presented earlier in this Chapter assumed a uniform temperature drop across the full section of the dam structure, for the purposes of simplicity. In reality, the surface zones will not experience as high peak temperatures during the hydration cycle, but will be exposed to significantly greater variations of seasonal temperatures during the operational life of the dam. The impact and influence of temperature gradients and differential cooling that will have consequently occurred across the section of Wolwedans Dam is investigated in this Chapter.

At 70 m in height and comprising approximately 200 000 m^3 of concrete, Wolwedans Dam is relatively small compared to many present-day RCC dams. However, the configuration of the structure is such that the core RCC is well thermally insulated in the lower parts of the wall, while the bulk of the upper part of the structure will be subject to surface zone temperature variations. In view of the fact that the dam arches and that the majority of this arching occurs in the upper part of the structure, it is considered important to gain an understanding of the different seasonal thermal cycles and the associated performance in all areas of the structure, and across the full section width. Only with such an understanding will it be possible to develop a realistic picture of the manner in which temperature affects the overall structural function.

5.4.2. INTRODUCTION

The comprehensive instrumentation and the fact that the dam has remained relatively consistently full since first filled in 1992[1 & 4], approximately 2 years after completion, implies that Wolwedans represents a particularly good source of information on which to basis the thermal/structural behaviour of RCC can be evaluated. The bulk of the hydration heat had dissipated from the body of Wolwedans only by late 1991, by which time the dam was impounded to 80% of full height, and accordingly, no data exists as to the extent of the induced joint openings without the influence of water loading.

In this analysis, the apparent thermal and shrinkage behaviour across and at different elevations on an RCC dam wall is investigated and the associated impact on the overall behaviour of the arch dam structure is reviewed. While the temperature cycles experienced across the section width will vary, dependent on the respective levels of thermal insulation, the influence of reduced insulation in the thinner, upper sections of the structure compared to the deeper, lower sections, is evaluated.

5.4.3. WOLWEDANS INSTRUMENTATION RECORDS

5.4.3.1. Instrumentation

The instrumentation installed and monitored at Wolwedans Dam is described in some detail in Chapter 2 of this study. For the purpose of the analysis addressed in this Chapter, temperature and displacement measurement at the long-base-strain-gauge-temperature-meters on each of the 4 levels of installed instrumentation were evaluated.

Plate 5.1: Wolwedans Dam Instrumentation Installation at RL 66.25 m

5.4.3.2. Data and Records

The temperature records for Wolwedans Dam indicate that the hydration heat had substantially been dissipated from the core of the dam wall in late 1991/early 1992[1, 3 & 4]. After that time, the temperature at the core of the structure has tended to follow a pattern of varying by approximately + 1°C in summer and – 1°C in winter around an average temperature of approximately 13.5°C.

In the surface zones of the structure, measured temperature variations are substantially larger, with summer maxima generally in the region of 20 – 21°C on the downstream side of the dam dropping to winter minima of approximately 11 to 13°C. Equivalent figures on the upstream side (under water) are 15 to 17°C and 12.5 to 13.5°C respectively.

In the core zones of the dam wall, the placement temperatures and the peak hydration temperatures averaged approximately 20 to 21°C and 30 to 33°C respectively, while the hydration heat was observed to be dissipated fairly immediately in the surface zones (within 2 m of the surface). Measurement in an intermediate zone, 5 m from the dam surface, indicated maximum hydration temperature rises of 3 to 4°C and subsequent

long-term variations of around 2.5°C around an average of approximately 15°C (i.e. higher than the core zone).

Table 5.3 summarises the zonal temperature variations recorded.

Table 5.3: Typical Zonal Extreme Temperatures

Zone	Seasonal Temperatures (°C)				Temperature Variations (°C)	
	Placement (T1)	Max Hydration (T2)	Max Summer	Min Winter (T4)	T2-T4	T1-T4
Core	20 - 21	30 - 33	14.5	12.5	17.5 - 20	7.5 – 8.5
External - upstream	20 – 21	21/24-26*	15 - 17	12.5 – 13.5	11.5 – 13.5	7.5 – 9.5
External - downstream	20 – 21	21/23-25*	20 - 21	11 - 13	10 - 14	7 - 10
Intermediate	20 - 21	23 – 25	16.25	13.75	9 - 11	7.5 – 8.5

* - maximum hydration temperature/maximum temperature.

It is important to note that although the hydration heat was rapidly dissipated from the surface zones and that the consequential maximum hydration temperature was low in these areas, the temperature was subsequently raised by the adjacent warmer internal RCC mass. By the same token, the temperature experienced in the external zones during the subsequent winter had dropped substantially, creating a significant differential between the external and the core zones (4 – 7°C).

The indicative differential temperatures are illustrated on **Figure 5.9** overleaf.

5.4.3.3. Joint Opening Profiles

Corresponding to the above "temperature zones", **Table 5.4** below lists the typical variations of the joint openings measured at Wolwedans at RL 66.25 m. See **Figure 5.6** for the locations of the listed joints.

As can be seen from **Table 5.4**, in the case of the open joints, the surface zone on the downstream face opens by between 0.2 and 0.5 mm more than at the core during winter despite experiencing similar minimum temperatures. During summer time, the joint openings on the same joints are similar in the core and the downstream surface zone, despite a temperature difference of around 6°C.

Annual temperature variations at the core of the dam structure of 2°C can be compared with downstream external zone variations of 7 to 10°C.

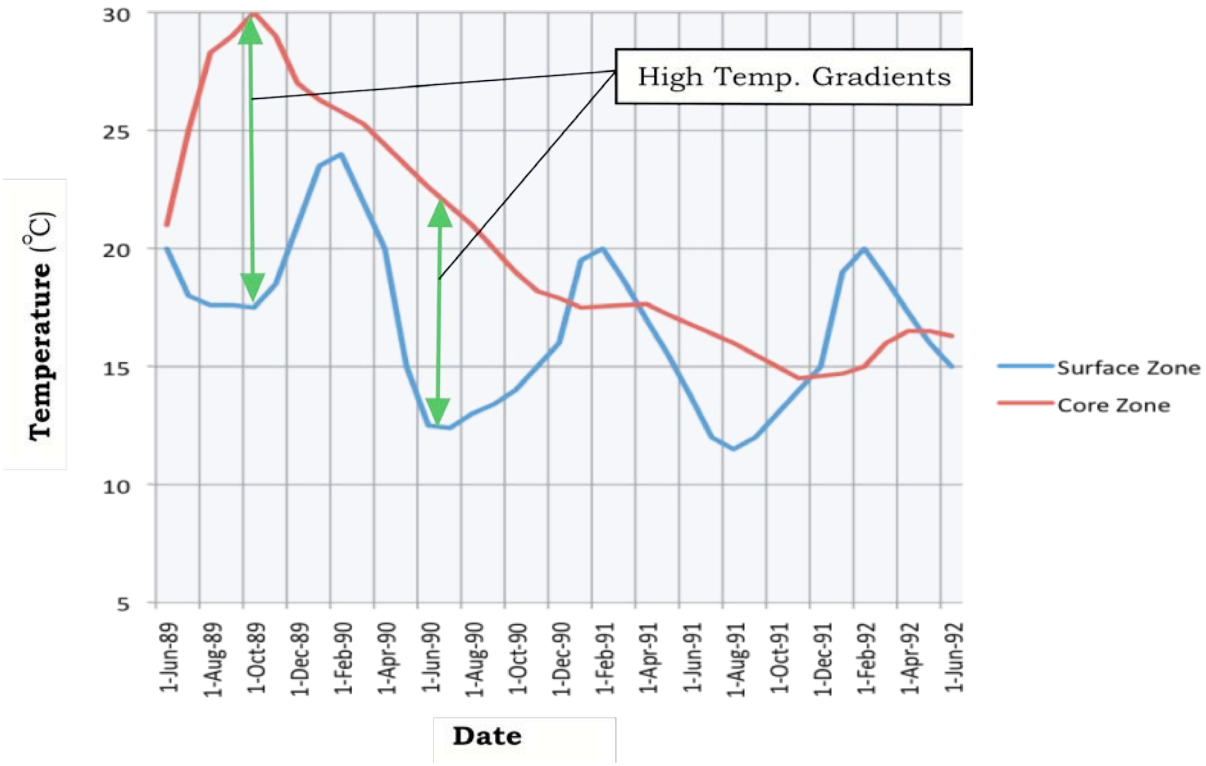

Figure 5.9: Typical Surface/External & Core Zone Temperature Histories(1)

Table 5.4: Maximum and Minimum Seasonal Joint Openings

Joint Nos.	**Surface Zone** (mm)				**Intermediate Zone** (mm)		**Core Zone** (mm)	
	Upstream		**Downstream**					
	Summer	Winter	Summer	Winter	Summer	Winter	Summer	Winter
7, 9, 10, 13, 15, 16, 19 & 22	0	0	-0.05	0.05	0	0	0	0
20	-0.15	-0.1	-0.1	0.05	0	0	0	0
11, 12	0.25	0.35	0.15	0.6	0	0	0	0
8	0.95	1.25	0.8	1.25	0.5	0.6	0.9	1.0
14	-	-	0.8	1.2	0.35	0.8	0.85	1.0
17	0.9	1.6	1.0	1.5	1.2	1.6	0.9	1.0
18	0.15	0.2	0	0.3	0.15	0.2	0	0
21	0.35	0.4	0.35	0.4	0.35	0.4	0	0.15

+ve indicates joint opening -ve indicates joint closing

The induced joints that remain closed indicate only a minor compression across the downstream surface zone in summer, which translates into a minor tension in winter.

In the upstream external zone, the observed joint openings do not indicate any real seasonal variation on the joints without any separation at the core. In the case of the open joints, the increased winter opening appears essentially equivalent to that apparent on the downstream, despite a reduced seasonal temperature variations of only approximately 3°C.

Reviewing the T1 – T4 temperature drop, similar values of approximately 8°C are indicated for both the core and intermediate zones, while a value of the order of 8.5 to 9°C is applicable for the external zones.

When reviewing the joint opening differences between the core and surface zones on the open joints and on the closed joints, it is important to consider the structural movement that will occur on these joints. When cold, the arch will tend to displace downstream, causing a closure between adjacent blocks at the upstream face and an opening at the downstream face. This was clearly evident on the structural analyses completed for Analysis 1 (parameters as per **Table 5.2**), where Joint 14, for example, indicated an opening of 0.1 mm at the upstream face, 0.77 mm on the centreline and 1.6 mm at the downstream face at RL 66.25 m.

5.4.3.4. RCC Temperature & Joint Behaviour at Elevation RL 84.25 m

In the top level of instrumentation at Wolwedans Dam (see **Figure 5.10**), the two LBSGTMs installed are within 2 m of the up- and downstream surfaces respectively (on either side of the gallery) and while the seasonal temperature variations experienced are typically 8°C on the downstream side and 2.5°C on the upstream side, the joints have never essentially opened, presumably as a consequence of the constant water load. Only at the extreme end of the right flank, at Joint 24, is any real displacement indicated. The fact that no arch action remains within the structure at this point confirms the fact that arch action is causing the complete closure of all of the other induced joints across the arch at this level.

In this upper area of the dam structure, the RCC placement temperature averaged approximately 22°C, the maximum hydration temperatures averaged 25 - 26°C and minimum winter temperatures experienced are approximately 13°C. With so little cover on these instruments from both the external faces of the dam and the gallery, they are effective entirely located in external zones.

With constant water load, the non-opening of the joints at RL 84.25 m implies that arch action is strongly and uniformly present in at least the top 15 m (below FSL) of the dam. This actually suggests stronger arching action than predicted by the finite element analysis modelling for design, which indicated that arching would be confined essentially to the spillway section and would be dissipated within 10 m below FSL.

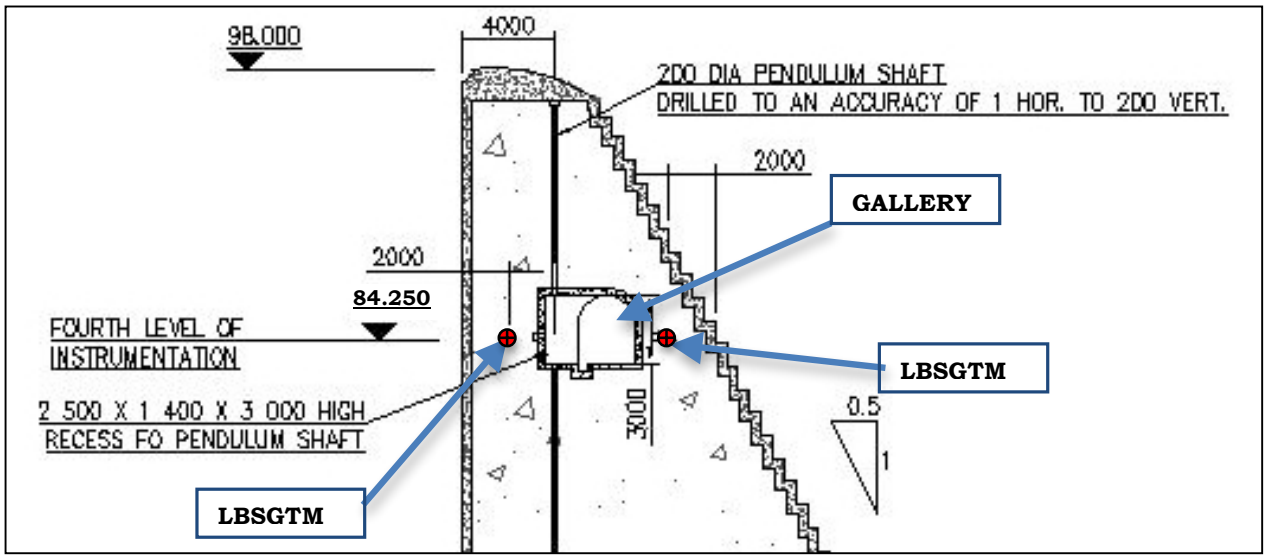

Figure 5.10: Typical Section of 4th Level (Top) Instrumentation at Wolwedans[1]

5.4.3.5. Core RCC Joint Openings

As previously mentioned, Wolwedans Dam first filled to capacity in early 1992, while at the bulk of the hydration heat had substantially been dissipated by late 1991/early 1992. From August 1991 to February 1992, the water level rose from 65% to 88% of full height. Subsequently, the water level rose slowly, but steadily for the remainder of 1992. Structural analysis revealed that arch action starts to develop in the dam wall at Wolwedans when the water level exceeds approximately 90% of the maximum service water level. This water level was reached during April 1992.

Examining the joint opening data, it is apparent that peak values were experienced during late 1991 and early 1992 and these were probably around 30% higher than the subsequent winter maxima. Summing the total maximum central joint openings at instrumentation level No. 3 (RL 66.25 m) during late 1991 indicates a total joint opening of approximately 4.7 mm, for a corresponding core temperature of approximately 14°C. Assuming a thermal expansivity of 10 x 10^{-6}/°C, a total joint opening of 4.7 mm would translate into an effective temperature drop across the 130 m long wall at this elevation of 3.6°C. Assuming that 25% of the shrinkage remained in the form of tensile stress would still only suggest an effective structural temperature drop of 4.5°C.

Comparing this situation with an analysis based on commonly accepted principles, it is possible to put the apparent performance of the RCC into perspective. For a shrinkage/creep volume reduction of 200 microstrain, a temperature drop of the order of 6°C to 14°C and a thermal expansivity of 10 x 10^{-6}/°C, total shrinkage of the order of 260 microstrain might be anticipated for the core RCC at Wolwedans. For a wall length of 130 m at RL 66.25 m and joint spacings at the centre of approximately

9.2 m, a total shrinkage of approximately 34 mm would equate to average joint openings of the order of 2.4 mm. Taken over the three joints that opened on the prototype, the full shrinkage across each joint would average more than 11 mm. The fact that the theoretical and measured joint openings are an order of magnitude different clearly demonstrates that the shrinkage and creep traditionally assumed for RCC in a dam did not materialise at Wolwedans Dam.

Either the shrinkage and the creep experienced under restrained expansion are substantially less than generally expected, or a very high level of creep must have been experienced in the RCC under tension. The latter hypothesis is considered extremely unlikely, as the compression strain is evident on all instrumented joints at Wolwedans and this compression tended to reduce to zero around mid 1990, which coincides with the time that the core temperature was equal to the placement temperature. If significant compression and tension creep had occurred, the compression strain would have reduced to zero substantially before the RCC cooled to the placement temperature and significant tensile strains would have been evident on joints that did not open, or more joints would have opened.

5.4.4. MODELLING OF OBSERVED DIFFERENTIALS

The instrumentation measurements demonstrate that the openings on the open joints are fairly even across all zones during summer, but that the external zones open on average approximately 0.3 mm more than the rest of the section during winter.

In an attempt to establish the implications of these apparent measurements, a simple thermal model of a single wedged 10 m block was set up and a temperature drop of 8°C was applied to the core and intermediate zones and 8, 9 and 12°C temperature drops were applied to the surface 3 m zones on the up- and downstream sides, with a thermal expansivity coefficient of 9 x 10^{-6}/°C, in a series of analyses. The block essentially represents a single block of the Wolwedans dam wall between induced joints at the elevation of the third set of instrumentation (RL 66.25 m).

For these analyses, the deformation along the length of one of the lateral block surfaces was evaluated.

The results of this analysis, as presented in **Figure 5.11**, indicated a lateral shrinkage of approximately 0.32 mm for the 8°C temperature drop, which was locally increased to 0.37 mm with an external surface temperature drop of 9°C and 0.50 mm with an external surface temperature drop of 12°C. The 12°C temperature drop accordingly indicated an increased external zone joint opening of approximately 0.36 mm (2 x (0.50 - 0.32)), suggesting that the external zone effectively experiences a larger effective temperature drop than the core zone of between 3 and 4°C. For a thermal expansivity of 10 x 10^{-6}/°C, the effective temperature drop differential would probably be 3°C.

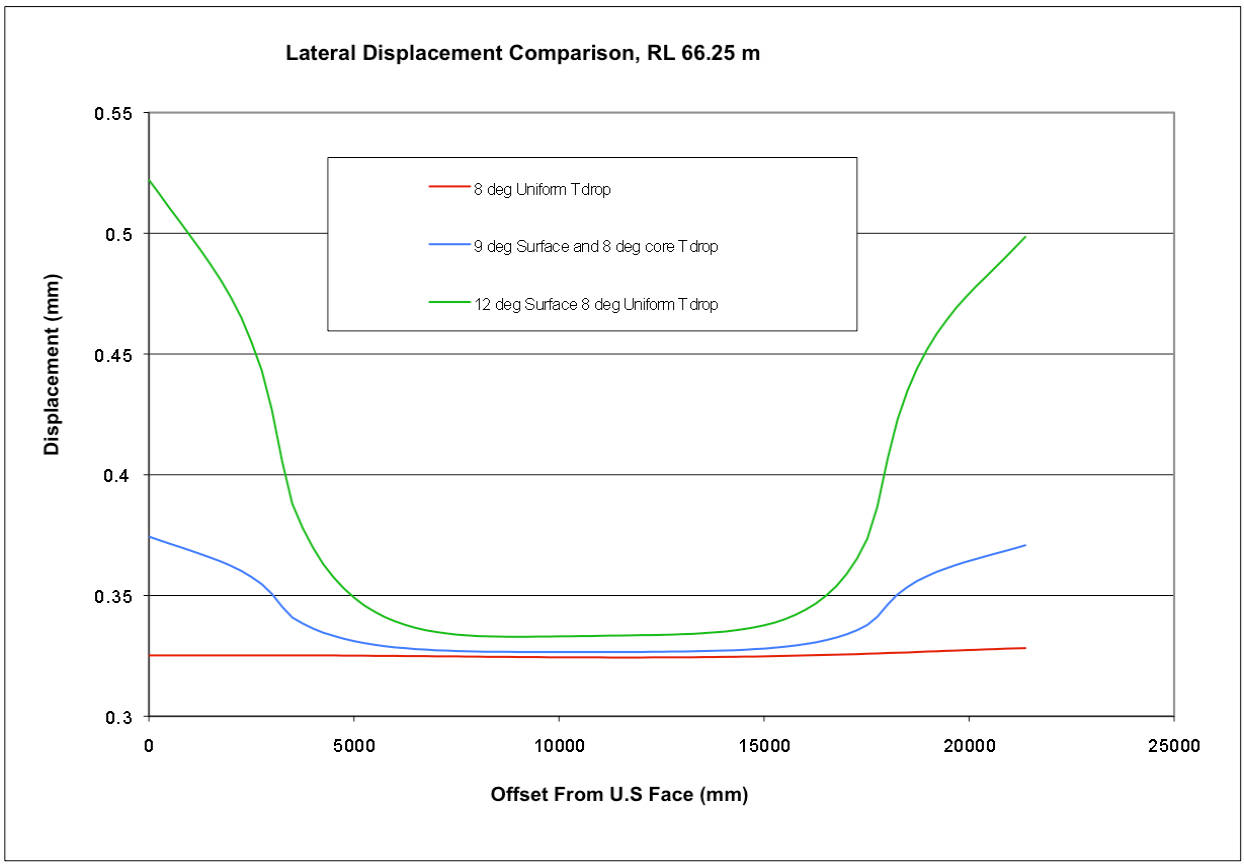

Figure 5.11: Displacement Profile for Differing Differential Temperatures

For a thermal expansivity of 10 x 10^{-6}/°C and a conservative long term elastic modulus of 20 GPa, a restrained 3°C temperature drop would give rise to a tension of 600 kPa, which would not be sufficient to exceed the RCC's horizontal tensile strength and explains why the closed joints would not experience the differential opening apparent on the open joints. However, the same logic suggests that the external zones of the dam would have been subject to a total effective temperature drop in winter of approximately 11°C. For a modulus of elasticity of 15 GPa, which is probably conservative, as much of the associated tensile stress would have occurred while the concrete was relatively young, a consequential maximum tension of 1.65 MPa would be developed. Considering the fact that the RCC of Wolwedans indicated an average core crushing strength of the order of 35 MPa, a horizontal tensile strength exceeding the apparent thermally induced tension could be anticipated, confirming the reason why surface zone cracking was not more generally apparent. On the other hand, it is considered unlikely that the effective differential temperature drop could exceed approximately 3°C, or there would have been more evidence of surface zone joint opening.

5.4.5. DISCUSSION OF WOLWEDANS DAM BEHAVIOUR

The instrumentation data for Wolwedans demonstrate that no real gain in temperature was experienced in the surface zones during the hydration cycle, although the heat in the adjacent core zone caused the temperature finally to be raised by between 2 and 6°C above the placement temperature. In the insulated core zone, a total temperature increase of the order of 10 to 12°C was experienced, while a heat gain of 3 to 4°C was experienced in the intermediate zone. Over the long term, the total temperature drop from the peak during hydration to the minimum during a cold winter can be seen to be of the order of 12°C and 20°C in the surface and core zones respectively.

The typical T1 – T4 temperature drop in the core zone and intermediate zones apparently increased by only approximately 1°C (8°C to 9°C) in the external zones, although distinct temperature gradients were developed between the zones during the first winter after placement.

At the open joints, the relative opening that occurs between summer and winter can be seen to increase from the core, to the intermediate, to the surface zone. The modelling undertaken suggests that the differential joint openings originate as a result of the fact that the total effective surface temperature drop experienced in the external zone is approximately 3°C higher than that experienced in the core zone.

This apparent behaviour suggests that some creep and/or micro-cracking must have occurred in the surface zones as a result of the temperature gradients experienced whilst the core zone was significantly heated with hydration energy and the surface was cooled during the winters of 1989 and 1990.

5.4.6. SUMMARY

The above review and analysis suggest that the application of a simple, linear temperature drop across the full arch section, as applied in the analyses described earlier in this Chapter, is not completely realistic and that thermal gradient effects gave rise to an effective maximum winter surface temperature drop of some 3°C more than was experienced within the core zone at Wolwedans.

For the purposes of the subsequent structural analyses of Wolwedans Dam, it is accordingly considered that it should be more accurate to apply a thermal loading more in line with that presented in **Figure 5.12**, although a verification of the validity of this pattern will only realistically be possible through 3-dimensional structural finite element modelling, as addressed subsequently in this Chapter.

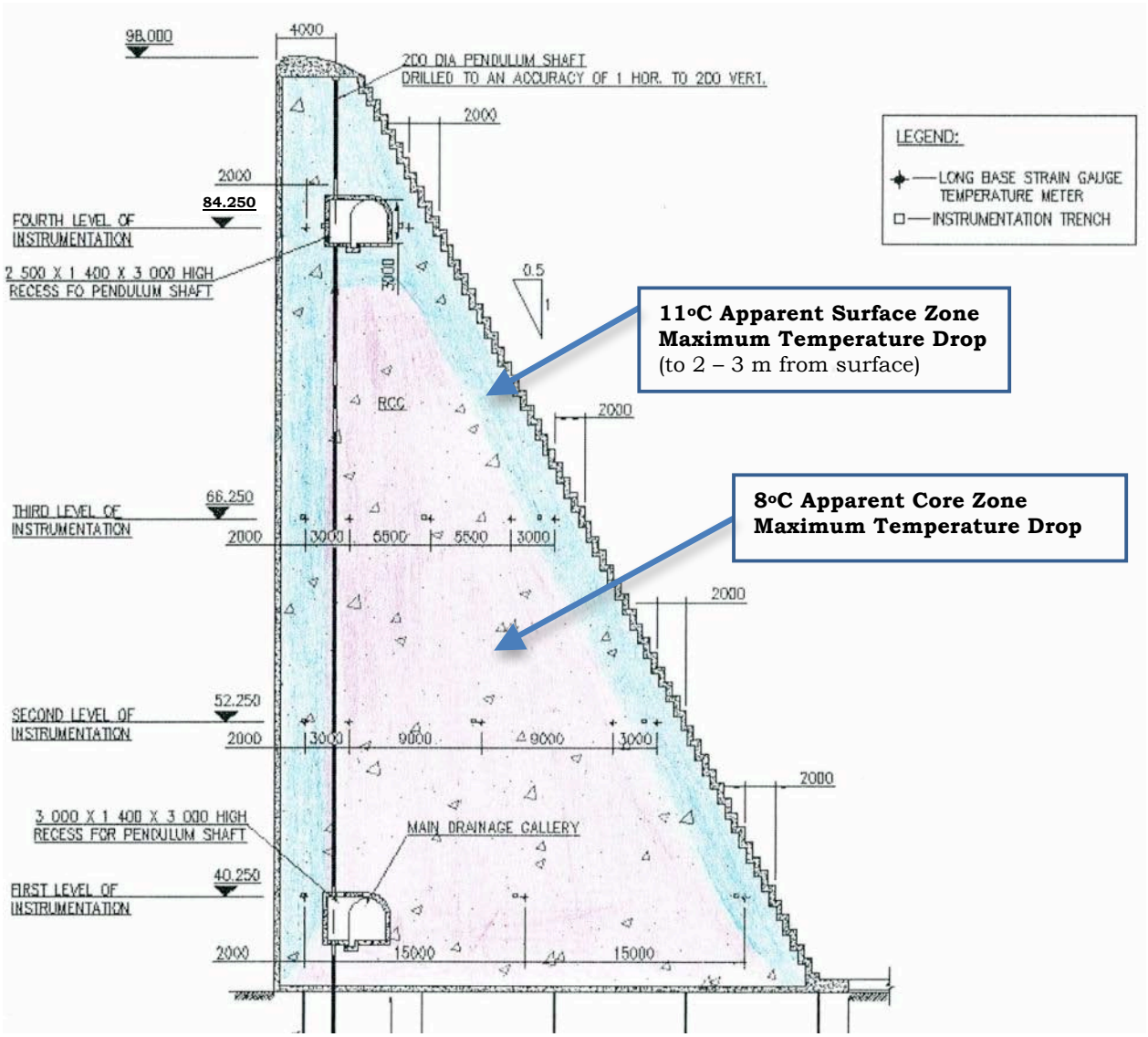

Figure 5.12: Apparent Effective Temperature Drop Distribution(1)

On the basis of the evaluation completed in this Chapter, it is considered that a greater knowledge of the influence of the differential cooling and associated temperature drop loads has been developed. Obviously, this phenomenon will indicate a variable level of influence, depending on the proportions of the structure in question. In view of the fact that most RCC arches will be relatively thin towards the crest, where the significant arching occurs, however, it is important to consider this effect when analysing all RCC dams with 3-dimensional stress transfer.

The understanding of the influence of differential temperature drops across the dam section developed through the above review is considered of benefit in respect of the detailed structural analysis of Wolwedans Dam, subsequently addressed.

5.5. ANALYSIS 3: MODELLING WOLWEDANS PROTOTYPE BEHAVIOUR

5.5.1. BACKGROUND

With the analyses described earlier in this Chapter providing a deeper understanding of the early thermal behaviour of the constituent RCC material and a greater confidence in the applicable pattern of temperature drop distributions within the dam body, it was considered appropriate to evaluate the behaviour of the dam structure as a whole, comparing modelled performance with measurements from the prototype.

In the case of an arch dam, the maximum crest displacements will vary significantly, dependent on the temperature drop applicable. Accordingly, comparing modelled and measured crest displacements for a range of effective temperature drops would allow the actual apparent temperature drop applicable on the prototype to be isolated with a high level of confidence. From an alternative perspective, applying a range of equivalent RCC shrinkage/creep volume reduction values, the materials behaviour that most closely reproduces the measured crest displacement and joint opening performance can be identified.

5.5.2. INTRODUCTION & OBJECTIVES

As presented earlier in this Chapter, the comparisons made on a specific level of installed instrumentation confirmed that RCC does not behave in the manner conventionally assumed. On the basis of maximum crest displacements, the analyses now addressed compare the overall structural performance measured on the prototype dam structure with that predicted by a Finite Element model for a range of shrinkage/creep scenarios.

In the text of this Chapter, only a summary of the findings of the described analysis is presented and the full investigation results are addressed in greater detail in **Appendix B**.

5.5.3. THE IMPACT OF TEMPERATURE DROP LOAD, OR SHRINKAGE ON ARCH ACTION

Before addressing in detail the Wolwedans Dam structural analysis, it is worthwhile to provide the reader with a background as to the significance of the modelling applied and accordingly the value of the results developed. For this purpose, it is particularly important to understand the influence of temperature drop loads and shrinkage on the function of an arch dam.

Temperature drop loads fundamentally impact the structural function of an arch dam as a consequence of the associated thermal shrinkage. While the associated impacts are described in detail in **Appendix A**, which is a partial extract from the author's Masters degree Thesis. 2001[13], a summary is provided in the subsequent text.

When subjected to depressed temperatures, the concrete of a dam structure obviously shrinks while the foundation rockmass remains unaffected. The net impact is a structure that is effectively marginally too small for its foundation and consequently tensions are experienced. Water load is transferred laterally in compression in an arch

dam into the abutments. When thermal shrinkage has resulted in tensile stresses in a similar direction, these must be overcome before arch compression can be re-established. When the water load is imposed on this structure under tension, increased arch and cantilever displacements must occur to close the tensile shrinkage and take up the load. With proximity to the foundation increasing structural stiffness within the dam wall, the displacement increases with distance from the foundation. Accordingly, the displacements on the arches and cantilevers are greatest in the centre and at the top of the structure, as indicated in **Figures 5.13** to **5.15**.

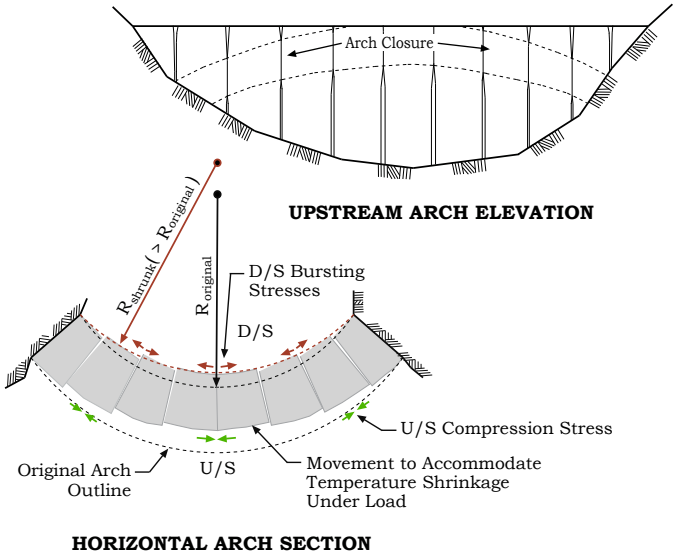

Figure 5.13: "Shrunk" Arch under Water Load

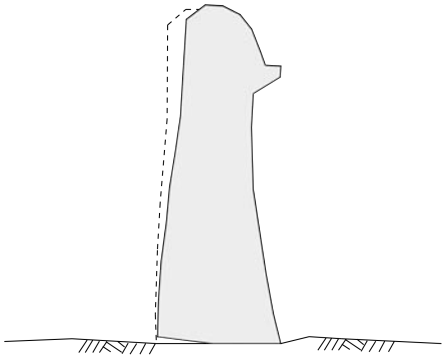

Figure 5.14: Deflection of Cantilevers

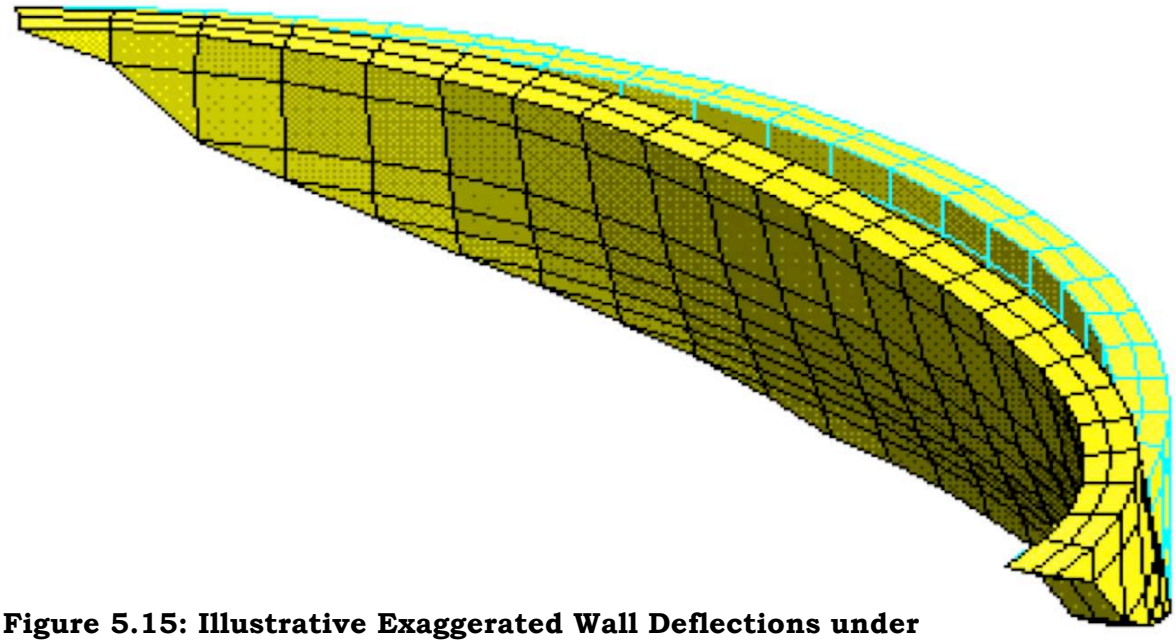

Figure 5.15: Illustrative Exaggerated Wall Deflections under Temperature Drop & Water Load

The above effect can substantially compromise the efficiency of arch action and this is addressed in **Appendix A**. Whether the result of creep, autogenous shrinkage, thermal shrinkage or a combination thereof, when an arch dam is subject to such shrinkage, the consequence is larger downstream displacements, increasing with distance from the foundation.

The importance of the above in respect of the analysis of Wolwedans Dam lies in the fact that increased shrinkage of the RCC will unavoidably be demonstrated in increased crest displacements on the arch structure. This is an impact that is unambiguous and cannot be disguised. The more "shrinkage" that occurred during the hydration heating and cooling cycle in the constituent RCC at Wolwedans Dam (due creep and autogenous shrinkage), the greater the measured crest displacements.

5.5.4. WOLWEDANS DAM INSTRUMENTATION RECORDS

5.5.4.1. Instrumentation

The instrumentation installed and monitored at Wolwedans Dam is described in some detail in Chapter 2 of this study. For the purpose of the analyses addressed in this Chapter, only the structural wall displacements and the joint openings at RL 66.25 m were considered alongside measured temperatures, with displacements being measured by geodetic survey and joint opening and temperature using long-base-strain-gauge-temperature meters. As a consequence of the spillway at Wolwedans being located in the centre of the dam wall, it is not possible to measure the maximum, central crest displacement, but only displacements on the non-overspill crests (NOCs). While the maximum crest displacements measured were accordingly at either end of the NOC adjacent to the spillway, displacement measurements from the upper gallery (at RL 85 m) covering the spillway section were available. Accordingly, it was considered that the behaviour of the prototype dam structure could be effectively defined through the displacements/deformations measured at the ends of the NOCs immediately adjacent to the spillway, three points within the upper gallery and the joint openings measured at RL 66.5 m on Joint Nos. 8, 14 and 17. The measurement positions on the dam structure are illustrated on **Figure 5.16**.

5.5.4.2. Geodetic Survey Instruments

Crest and other displacements are measured at Wolwedans Dam twice a year[7], in late January, or early February and in August, on the basis of taking measurements when the dam structure experiences its maximum and minimum temperatures. Measured data for the period January 1990 to August 2008 was provided to the author by the Spatial & Land Information Directorate of the Department of Water Affairs & Forestry (see **Appendix B**). To correspond with the temperature and joint opening data available to the author, specific attention was paid to the displacement data for the period 1990 to 1996, with the coldest temperatures within the dam structure during that time being measured in August 1995. At this time, the temperature within the core of the dam structure measured approximately 13 - 14°C.

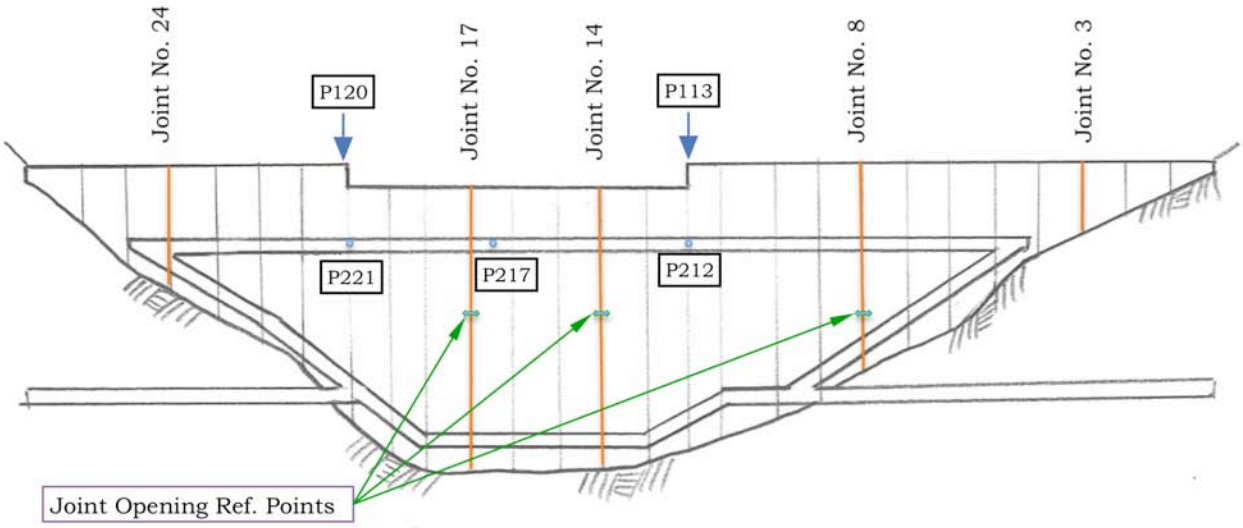

Figure 5.16: An Illustration of the Measurement Reference Points on Wolwedans Dam (viewed from Downstream)

Compared to 1995, the winter temperatures of 1993 were almost as cold, but at that time, the induced joints had not been grouted. This implies that the displacement measurements for 1993 can be more easily interpreted, without having to hypothesise any potential impacts consequential to joint grouting.

5.5.4.3. Induced Joint Grouting

Grouting of the induced joints at Wolwedans Dam is addressed in a DWAF report[14] and summarised in a technical paper presented at the Santander RCC symposium in 1995[15]. The induced joints at Wolwedans Dam were grouted in two phases between June and November 1993. The first phase encompassed grouting of the structure from the base to mid-height and was completed during the winter months of June to August. The impounded water level was reduced over this period, reaching a minimum of 8 m below FSL. The second phase of grouting, from mid-height to crest level, was undertaken during the Spring and early summer months of September to November, during which time the impoundment was at full capacity.

Studying the deformation data records over the period that grouting was undertaken at Wolwedans Dam, a number of significant observations can be made, as follows:

- On July 3rd 1993, early during the grouting exercise, a total downstream horizontal crest displacement (compared to January 1990) of 14.4 mm was measured at the end of the left flank NOC, at which time the impoundment was almost full.

- Lowering the impoundment water level by 8 m during the first phase grouting operations gave rise to an upstream movement of the crest of the order of 2.5 mm and an equivalent upstream movement at the upper gallery level of

approximately 0.5 mm. No similar effect could be discerned in the form of induced joint opening, or closing at any of the instrumentation levels.

- A net upstream movement of the dam crest of approximately 2.5 mm was recorded in February 1994, compared to February 1993, despite a 2 m higher impounded water level. This suggests that the grouting caused an upstream movement of the crest towards the centre of the dam of approximately 3 mm.
- Of the 58 instrumentation sections, across four levels, the impact of the joint grouting is only really discernable at three (as indicated on **Figures 5.17**, **5.18** and **5.19**) in the form of reduced seasonal joint movement.
- At the time of grouting, the only induced joint to have opened above RL 84.25 m was Joint No 24 (at the far end of the right flank).
- The only joint at which a distinct and definitive impact of the grouting was apparent was Joint No. 24, which demonstrated significantly reduced movement after grouting (see **Figure 5.19**).

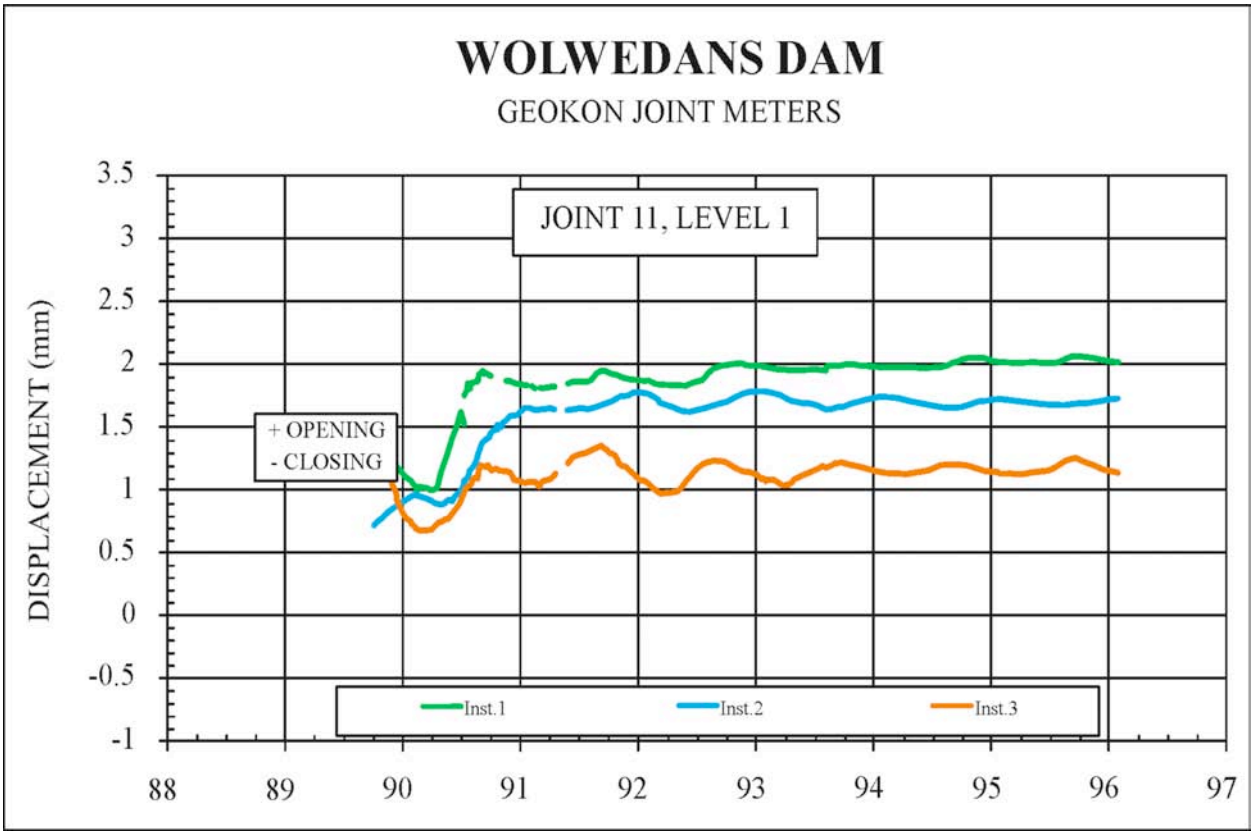

Figure 5.17: Displacement History for Joint No 11 at RL 40.25 m[7]

It is considered particularly significant that the behaviour of joint Nos 11 and 24 appeared to be impacted most obviously by grouting, as these were also the joints that indicated the most significant opening. Grout penetration of the induced cracks was obviously most successful on these joints.

It is also particularly interesting to note that the behaviour of the dam structure after grouting has changed substantially more in the warmth of summer than in the cold of winter and this is easily explained.

In the case of a CVC arch dam, the hydration heat is artificially dissipated and the concrete temperature is usually further depressed while the dam is empty and before any hydrostatic loading is imposed. In this process, the monolithic blocks in which the dam is constructed shrink away from each other, with the resultant gap between blocks increasing with distance from the foundation restraint. The gap between blocks is subsequently filled with grout and the continuity of the structure between the abutments is re-established at the temperature at which grouting is undertaken (see **Appendix A**). By grouting at, or close to, the coldest operational temperature, the dam structure would never subsequently suffer from any significant temperature drop loading, but only increased temperatures that will increase arch stresses.

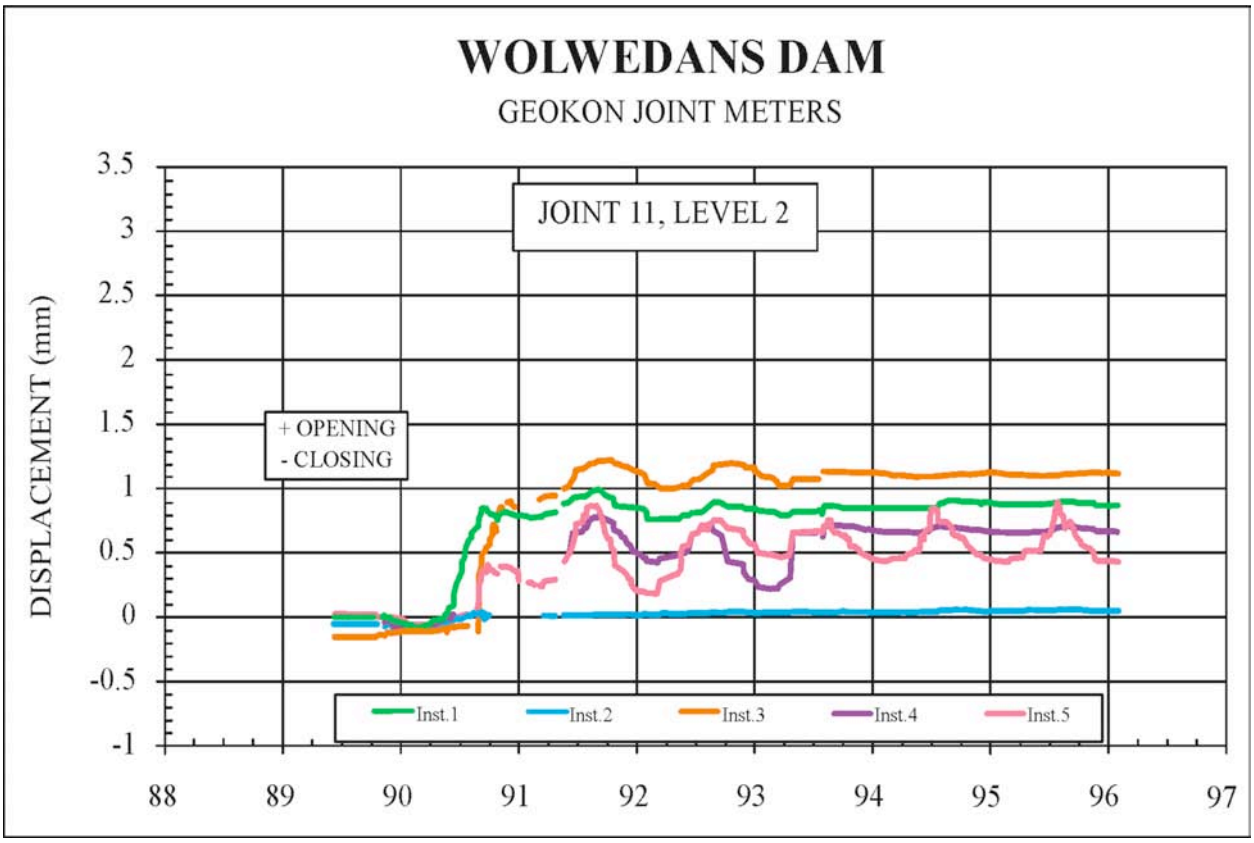

Figure 5.18: Displacement History for Joint No 11 at RL 52.25 m[7]

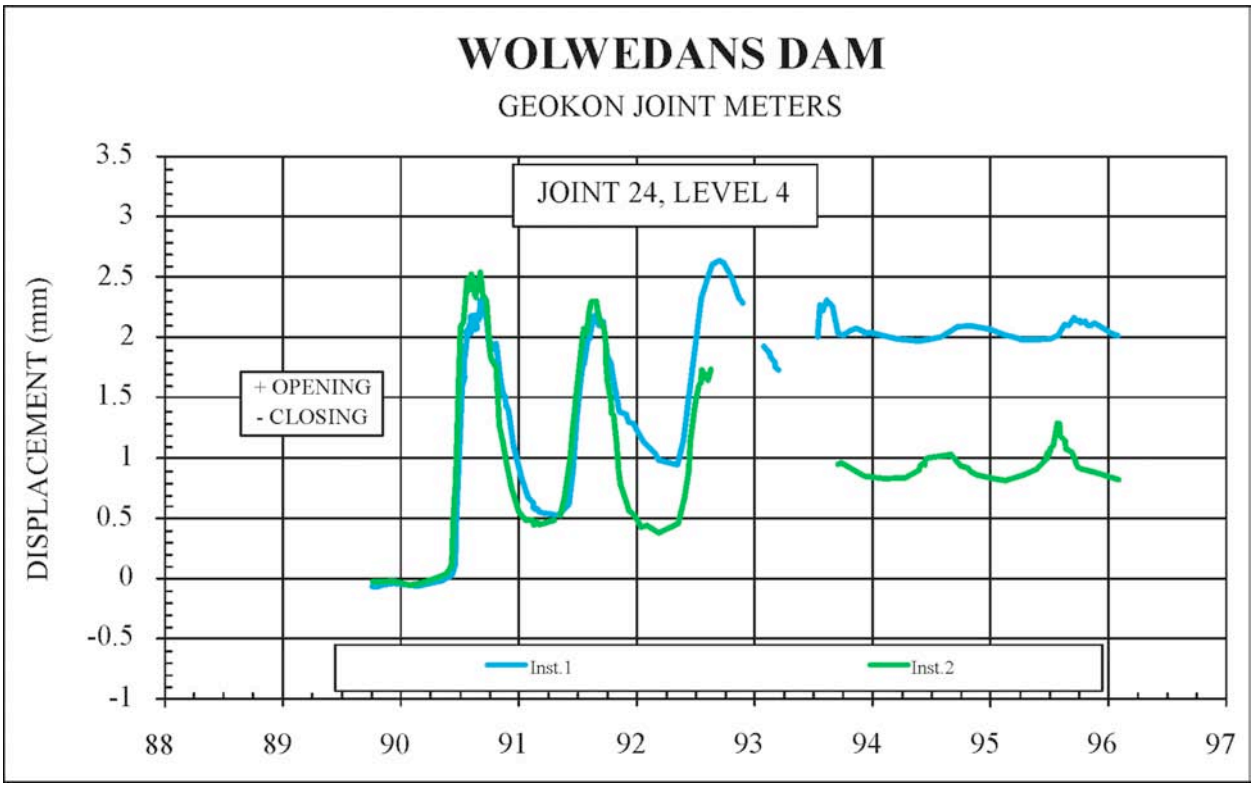

Figure 5.19: Displacement History for Joint No 24 at RL 84.25 m[7]

In the case of Wolwedans Dam, however, the dam structure had been carrying the full hydrostatic load for a while by the time that the full temperature drop load had developed. Observing only a single induced joint open at elevation RL 84.25 m is indicative of the fact that the hydrostatic loading had caused sustained arch compression stresses at this level of the dam (and above) since first impoundment. A crack was observed at Joint No. 24 as this area of the dam falls outside the section that carries arch stresses. At the time of grouting, the dam was accordingly shrunk by temperature drop, with arching limited to the upper zones of the structure and the induced joints tending to be open in the lower parts of the structure, as the shrunk cantilevers are too stiff to adequately deform and transfer stress laterally.

During grouting, it is obviously the open joints that are most effectively filled with grout. Where the structure has no open joints and transfers compression arch stresses, very little grout penetration of the joints would have been achieved. Consequently, the dam structure was effectively simply grouted up in its deformed shape. The areas most successfully grouted are those of least importance in respect of the impact of a temperature drop load and those areas least successfully grouted are conversely the most important.

The above situation is borne out by the fact that the dam structure displaces further upstream under the influence of the warmth of the summer months than previously, but no less far downstream during winter cooling. With the induced joints wherever previously open now filled with grout in a cold winter, any subsequent temperature

increases will cause expansion, resulting in the structure tending to bulge in an upstream direction.

5.5.4.4. Interpretation of Crest Displacement Measurements

The base survey data for the geodetic displacements at Wolwedans was recorded in January 1990, soon after the dam was completed, but before impoundment. The data was then translated to a zero reference in August 1992, when the dam first filled. Before examining the crest displacements measured, it is important to attempt to establish the absolute zero reference displacements. At the time of the first geodetic survey, the dam wall had essentially just been completed and the temperature within the structure was elevated. This would cause the empty dam to lift and displace upstream. Furthermore, under gravity load alone, the empty structure will tend to lean towards the upstream, with the highest bearing stress under the heel, and an upstream crest displacement would result. As cooling of the hydration heat subsequently occurred, the dam was filling and accordingly it was not possible to gain a clear picture of the crest movement that related specifically to temperature alone.

The picture related to the crest displacement behaviour is further clouded by two other factors; the fact that the upstream displacements apparently increased when the dam was full to around 2/3 height during the summer of 1991 and the fact that the placement and equilibrium temperatures in the dam structure undoubtedly increased towards the right flank. Both of these issues probably relate directly to the same climatic effects. The upstream face of Wolwedans Dam faces almost directly north and the top 30 m of the upstream face was probably warmed by particularly intense solar radiation during the summer of early 1991 before the dam filled. Similarly, the right flank of the dam and the right abutment rockmass would be exposed to direct sunlight early and through the warmest part of the day, whereas the left flank would only start receiving solar radiation later in the day, when the intensity has significantly diminished. The impact of the latter effect is tangible and the instrumentation at RL 84.25 m demonstrates typical seasonal temperature variations in the concrete between 12.5 to 21°C on the left flank that can be compared directly with equivalent variations of 14 to 23.5°C on the right flank (see **Figure 5.20** and **5.21**).

However, despite an apparent increased upstream movement of the crest in 1991 compared to 1990 of between 1.5 and 2 mm, instrumentation at RL 84.25 m clearly indicated a net drop in temperature of 3 to 4°C, which could further be seen in a general downward movement of the crest by approximately 3 mm. Furthermore, although the dam has been consistently full since late 1992, similar upstream displacements as those evident when the dam was empty and warmed by hydration have apparently been experienced occasionally since, specifically on the right flank. Instrumentation at level RL 84.25 m indicates that the temperature of the upper section of the dam typically varies on an annual cycle from approximately 13 to 22°C, which corresponds with a measured displacement variation range of between 10 and 13 mm on the dam non-overspill crest and 4 to 6 mm at the central monitoring points within the upper gallery.

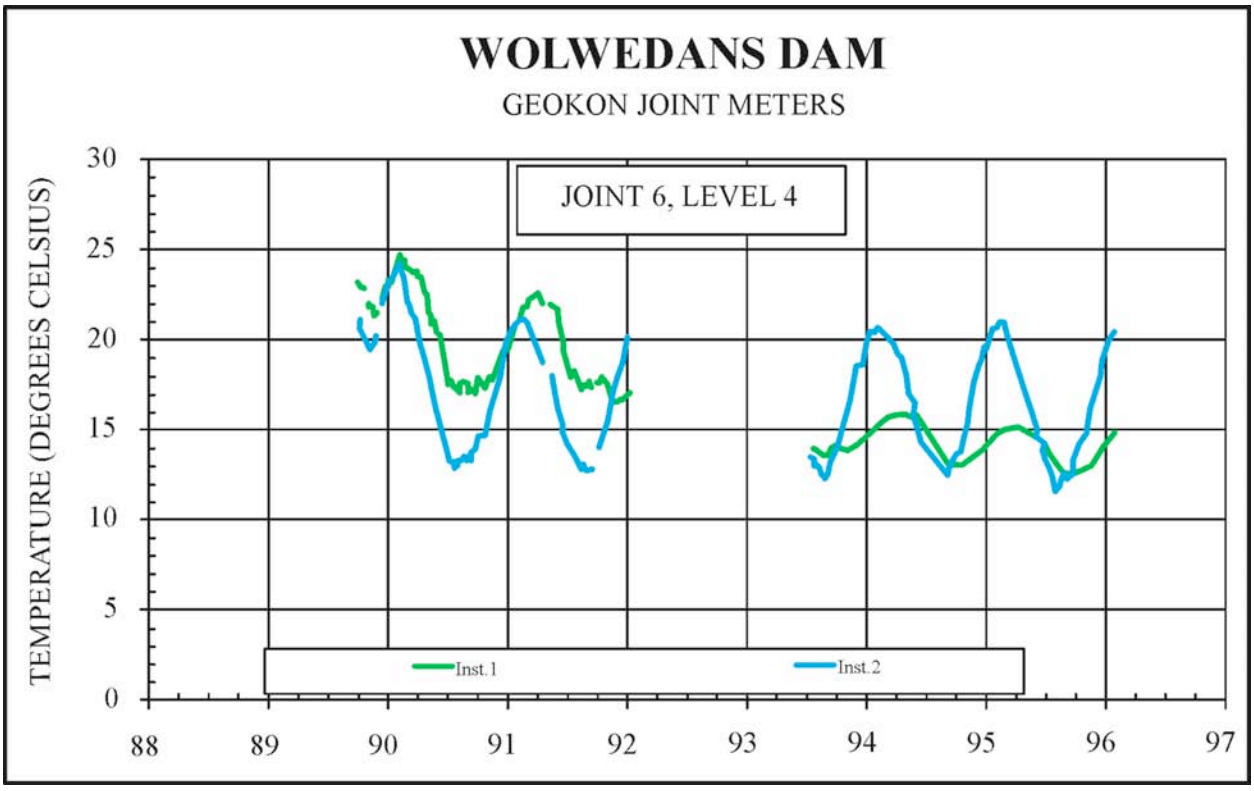

Figure 5.20: Typical Temperature History at RL 84.25 m on Left Flank[7]

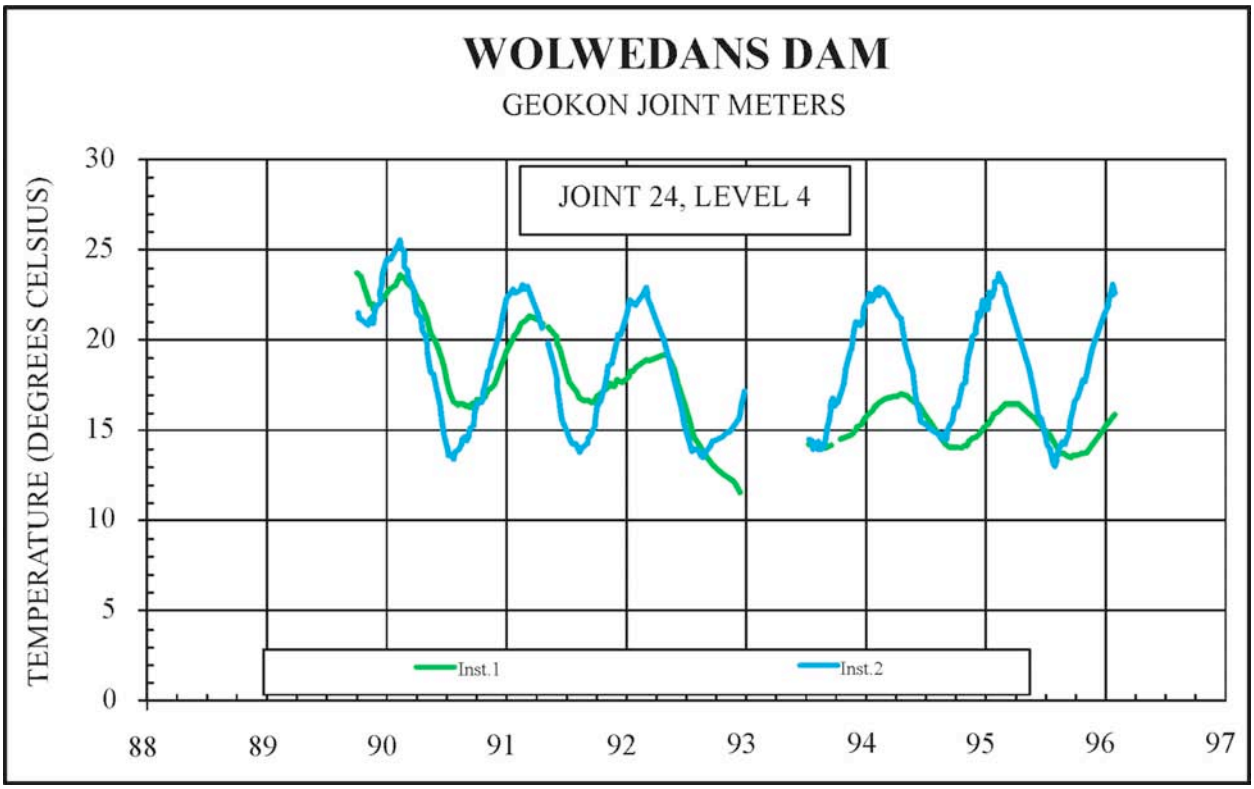

Figure 5.21: Typical Temperature History at RL 84.25 m on Right Flank[7]

It should be noted that throughout the parts of the Wolwedans Dam structure for which data exists, even the warmest temperatures experienced during the typical seasonal cycle are lower than the equivalent placement temperatures.

Reviewing the temperature data in January 1990, it would seem that the temperature of the section of the dam below RL 48 m (which was placed during 1988) was actually depressed by around 3°C below the average placement temperature, while the temperature of the RCC placed during 1989 (RL 48 – 103 m) was raised by between 2 and 3°C above the average placement temperature. Inputting this information into the finite element model, with gravity loading but without water load, indicated that the dam crest at the NOC on either side of the spillway would displace upstream by between 3.5 and 5 mm compared to its "zero temperature" state. Under water loading, this upstream displacement would be translated into a net downstream displacement. Considering the fact that the net temperature changes from placement should subsequently almost always be temperature drops, it is very surprising to observe an apparent, large upstream movement, as evident on the right flank.

Reviewing the seasonal temperature histories at elevation RL 84.25 m, the insulating effect of the impounded water is clearly demonstrated through a significantly greater temperature variation range on the downstream side, compared to the upstream. Within the NOC, however, no water insulation will be present and, with greater exposure to solar radiation, the upstream and top sides will experience higher temperatures during summer than the downstream side. With just a 5 m wide section and greater exposure to climatic effects (on 3 surfaces), it is considered certain that the temperature variations experienced within the NOC will consequently exceed those at the upper gallery level and it is very likely that the Non Overspill Crest of the dam correspondingly experiences temperatures above placement during the warmest summer months, particularly on the right flank. The fact that the only joint to open (No 24) on the right flank was successfully grouted will further increase the tendency of the right flank crest to indicate upstream movement during periods of particularly warm temperatures.

This issue is also addressed in **Appendix B** and the pattern of movement of the right flank of the dam is reviewed in more detail and in tandem with the seasonal rockmass movements. It is concluded that the most likely cause of the apparent additional upstream crest movements of between 3 and 7 mm on the right flank of the dam is higher summer season increases in temperature, both within the affected upper section of the dam structure and in the abutment rockmass on the right flank. However, it is recognised that ascertaining real certainty in respect of these observed phenomena was not possible within the scope of the work addressed in this study and consequently, less credibility and importance was placed in the accurate replication of displacements on the right flank of the dam.

In respect of the overall displacements measured on the prototype dam structure, the impact of the induced joint grouting exercise is difficult to determine with certainty. While the data would tend to suggest that a net upstream summer movement of the

upper part of the dam was incurred through the grouting, the total downstream displacements in winter seem unaffected. This observed behaviour is consistent with a hypothesis that the open sections of the induced joints of the cooled dam structure were filled with grout, while no grouting was really achieved in the areas under structural compression at the time of the grouting exercise, where the joints were closed. In terms of long-term behaviour, this implies that the grouting exercise did not drop the "zero stress" temperature as intended and that the same temperature drop load as before grouting will be applicable.

On the basis of the various uncertainties, it is considered that the most reliable data sets, in respect of structural displacements, are the displacements measured from January 1990 to July 1993 and the seasonal displacement variations.

5.5.4.5. Crest Displacement Measurements

Measurement points P113 and P120 are located at the beacons on the NOC immediately to the left and right sides of the spillway at Wolwedans Dam, respectively. The total horizontal, downstream crest displacement measured at these beacons in July 1993 was recorded as 14.5 and 11.7 mm respectively, compared to a base reference of January 1990. Equivalent seasonal displacement variations at these two points are approximately 10.9 and 12.8 mm respectively. While the data from the reference point P113 appears consistent with expectations, the seasonal variations and the total displacements indicated for point P120 are substantially higher than anticipated.

Plate 5.2: Wolwedans Dam – Illustrating Crest Beacons P113 & P120

5.5.4.6. Discussion on Measured Displacements

The spillway of Wolwedans Dam is located closer to the right flank than to the left, effectively as a result of the steepness of the right abutment (see **Figure 5.22**). However, while the dam height is also less at the point of the start of the NOC on the

right flank, compared to the left, the inlet tower is situated close the start of the NOC on the left flank. In order to establish the stiffening effect of the inlet tower, a series of analyses with and without the tower were run. While these indicated that the tower resulted in reduced displacements across the full arch, the impact was marginal, with displacements only reduced by slightly more than 1% at the end of the left flank NOC. However, where the surveyed displacements on the crest to the right side of the spillway were generally 15 to 20% lower than the equivalent values recorded on the left flank, the FE model un-surprisingly predicted that displacement on the right flank at P120 should be approximately 60% of that on the left flank at P113.

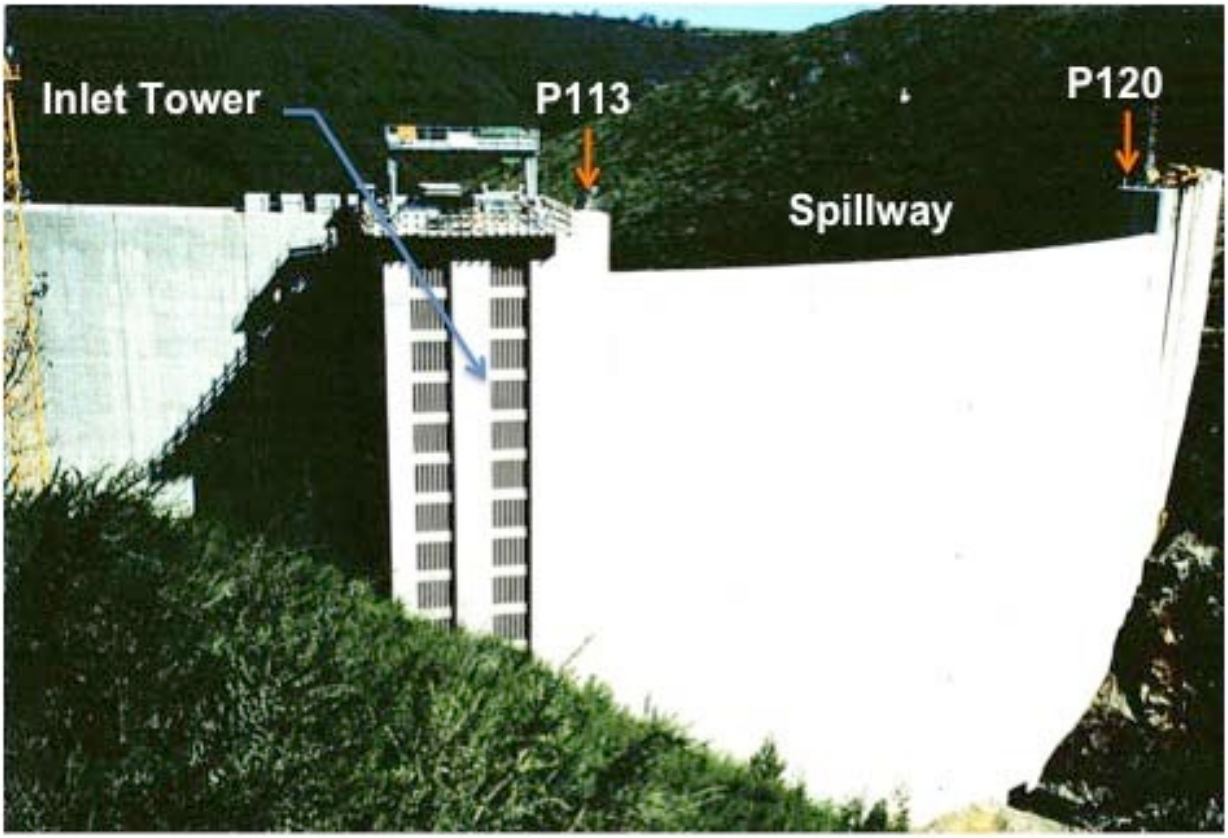

Plate 5.3: Upstream View of Dam Illustrating Beacons, Tower & Spillway

It is not possible to discern any specific related patterns in the survey data over the past 20 years that might explain this anomaly and the displacements appear equally elastic on both flanks.

The issue of the unexpectedly high upstream crest displacements on the right flank is discussed in more detail in **Appendix B** and it would appear that temperature rises in the right flank rockmass may also contribute to the observed movements. No similar movement can be discerned in the induced joints at the upper gallery level, which all remain closed at all times.

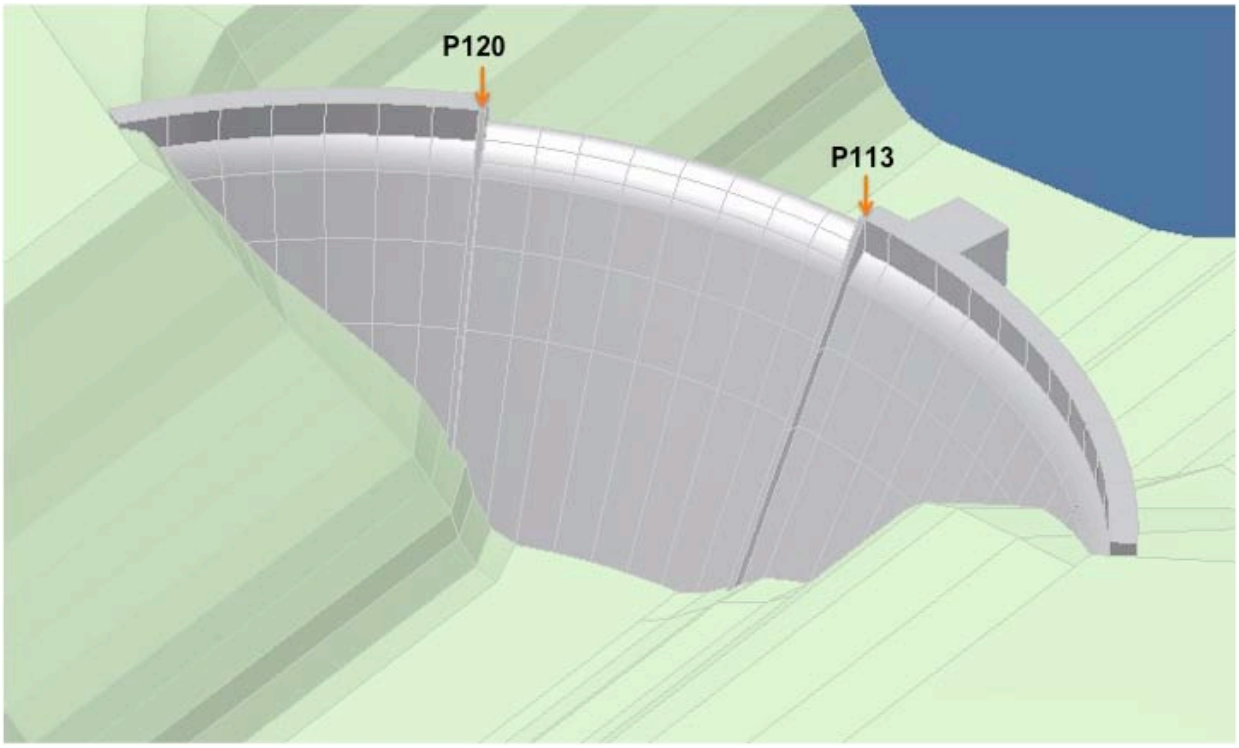

Figure 5.22: FE Model Illustrating Crest Displacement Monitoring Points

5.5.4.7. Displacement Measurements in the Upper Gallery

Due to the fact that the displacement measurement within the upper gallery at Wolwedans Dam was only initiated in August 1992, it is not possible to establish a "zero" reference for this data with real confidence. The measured data within the gallery, however, can be seen to be very consistent, with displacement increasing in line with expectations with distance from the abutments, although unexpectedly high displacement variations on the right flank are again evident. The manner in which the measured data was adjusted to a "zero" reference is discussed in **Appendix B** and the approach applied implies that the prototype reference displacements almost certainly conservatively overestimate the reality.

5.5.5. PROTOTYPE REFERENCE BEHAVIOUR

On the basis of the above, the data listed in **Table 5.5** for July 1993 was defined as the target reference behaviour for the prototype Wolwedans Dam under a nominal core 8°C temperature drop from placement temperature.

Table 5.5: Measured Displacement Data at Reference Points 1993 (mm)[7]

Reference Point	**113**	**120**	**212**	**217**	**221**
Reference Horizontal Downstream Displacement	14.5	11.7*	7.65	10.1	7.5*
Seasonal Variations 1993	8.0	10.5*	3.2	4.5	3.5

Induced Joint No.	**8**	**14**	**17**	Total
Central Opening at RL 66.25 m July 1993 (mm)	1.0	0.95	1.45	3.40

The data indicated with an asterisk (*) is located on the right flank and viewed with reduced confidence.

5.5.6. DAM STRUCTURE DISPLACEMENT MODELLING

5.5.6.1. Background & Objectives

The objective of the analyses addressed in this Chapter is to compare the overall structural performance of the Wolwedans arch/gravity dam wall, as measured on the prototype through crest displacement and joint opening, with a range of RCC shrinkage/creep materials models through simulation using Finite Element analysis.

For the early behaviour assumed for RCC, or the "Traditional RCC Materials Model" it would be usual to assume a "typical" total effective volume reduction of approximately 200 microstrain due to shrinkage and creep during the hydration heating and cooling cycle, as discussed in Chapter 3. If a further temperature drop of the order of 8°C to the long-term minimum core body temperature is assumed, at a thermal expansivity of 10 x 10^{-6}/°C, the total post-placement volume reduction, or shrinkage would consequently equate to 280 microstrain.

In reviewing the analyses undertaken, it must be recognised that the modelling presented can never be anything more than an approximation of the reality. As discussed in Chapter 3, due to the complex elastic and inelastic behaviour of concrete, the influences of seasonal and site-specific placement temperature variations, varying degrees of internal restraint caused by the size of the structure in question, differential stiffness values across the foundation rockmass, etc, an evaluation of the early behaviour of RCC within a dam can be regarded as an estimation at best. However, the traditional theory and the conventional approach to dam design assumes a volume reduction of the order of 200 microstrain as a consequence of creep (and autogenous shrinkage) during the hydration heating and cooling cycle and this will have an impact on the structural behaviour of the dam that should be very obvious.

The objective of the analysis undertaken was accordingly not to precisely identify the actual behaviour mode of the dam and its constituent materials, but to establish the nature of the performance that would have been expected on the basis of the

traditional design approach and assumed materials characteristics for RCC and to compare the actual performance with a number of possible RCC behaviour scenarios.

It is, however, considered particularly important to take note that the structural modelling is attempting to reproduce crest displacements and induced joint openings. Having opened due to a temperature drop and possibly creep during the hydration heating and cooling cycle, the induced joints close under the water load as the separated cantilevers (between open induced joints) displace forward and make contact at the crest to develop arch action. The higher the E modulus applied for the RCC, the less the cantilevers deflect, the lower the total crest displacement and the wider the induced joints remain open. Consequently, while it is possible to assume some creep in conjunction with a higher E modulus for the RCC in order to reproduce the measured crest displacements, the higher E value will result in reduced closure of the induced joints, while the joint openings will also have been increased by the creep. The consequence would be the prediction of substantially greater induced joint openings than measured in reality. Accordingly, matching the measured induced joint openings and the crest displacements will require a reasonably realistic simulation of the actual RCC behaviour.

5.5.6.2. Earlier Analyses

The Wolwedans Dam arch/gravity RCC dam structure was modelled as part of the first dam safety evaluation, completed in 1997, 5 years after full impoundment was first achieved. This work is summarized in the Department of Water Affairs and Forestry report "3-D Structural Analysis of Wolwedans Dam"[16]. This study, which was relatively simplistic in nature, demonstrated that a maximum, central crest displacement of approximately 4 mm under (FSL) normal hydrostatic loading was increased to approximately 12 mm when a uniform 6°C temperature drop was applied to the complete structure.

This analysis was undertaken using three different FE analysis programs; ABAQUS, ANSYS and NISA. For the same material properties, element meshes and load cases, the maximum horizontal crest displacements indicated by each of the three programs varied by approximately 12%, while the maximum toe stresses presented varied by over 50% and the maximum heel tensions by over 25%, providing an indication of the divergence in analysis result presentation typically evident for different FE analysis systems and models, particularly at discontinuities. While the actual FE analytical processes cannot differ between the various different software versions, the divergence in output is found in the manner and precise location within each element that the stresses are indicated.

An analysis with the same geometry, materials properties and loadings was repeated as part of this investigation using COSMOS[8] and the maximum indicated in-stream crest displacement was 4.6 mm, which was approximately 5% higher than the highest value for the other three programs. While the analysis completed as part of this study used a denser mesh with tetrahedral elements, the results serve to confirm the

COSMOS user manual's assertion that the program is conservative and will generally present displacements and stresses that are on the higher side, when compared with a typical range of FE analysis systems. While this again relates to the particular approach taken by COSMOS to the presentation of output from the model elements, it is stated here simply to recognise an additional factor of conservatism in the analysis results presented.

5.5.6.3. Modelling the Wolwedans Dam RCC Arch/Gravity Structure

Analysis Methodology

To maintain the approach applied for the earlier analyses, only linear-elastic FE modelling was undertaken. While this is not considered completely realistic, as the increased cantilever displacements are highly likely to give rise to plastic deformation as tensions develop at the heel, it is a conservative, tending to result in underestimated crest displacements on the model.

While the materials behaviour to be modelled relates to shrinkage caused by creep during the hydration process, as well possibly as early autogenous shrinkage, these can best be simulated as elastic shrinkage caused entirely by a temperature drop. Accordingly, the 280 microstrain shrinkage that the conventional approach (traditional RCC materials model) would suggest occurs in mass RCC would be simulated on the FE model by applying a temperature drop of 28°C at a coefficient of expansion of 10 x 10^{-6}/°C.

For each of the behaviour scenarios analysed, the in-plane displacements on the crest on either side of the spillway and at the strategic locations in the upper gallery were noted, together with the central joint opening predicted on open Induced Joint Nos. 8, 14 and 17 at elevation RL 66.25 m.

Materials Properties & Loadings

It is acknowledged that it would never be possible to precisely establish the actual mechanical properties of the dam RCC and its foundation rockmass and that it would be possible to produce an almost limitless quantity of analysis results, depending on the combination of E values, coefficients of thermal expansion, uplift load and effective temperature drop applied. However, reproducing induced joint openings and crest displacements that both reasonably accurately correspond to the measured values does narrow the possible materials property and loading variations.

For the purposes of the analysis presented herein, the measured materials properties for the RCC of Wolwedans Dam[1] and those properties and characteristics demonstrated through modelling in the first set of analyses presented in this Chapter to be most valid were applied for the analyses addressed. These and the loadings that were considered as constant are summarised in **Table 5.6**. At the time that the critical displacement values were measured in July 1993, the impounded water level was

recorded as just 300 mm below FSL and accordingly, hydrostatic loading equivalent to water storage at the Full Supply Level was applied for all comparative analyses.

In order to demonstrate the validity, or the apparent representivity, of the selected materials properties a sensitivity analysis was also completed, applying a higher E modulus value (25 GPa) for the RCC in conjunction with some creep (30 and 50 microstrain).

Table 5.6: Materials Properties & Constant Loads Applied for All Analyses

Property	**Value Applied**	**Loading**	**Value Applied**
RCC Density	2400 kg/m^3	Hydrostatic	FSL (RL 98 m)
RCC Compressive strength	35 MPa	Uplift*	50% Design
RCC Elastic Modulus (sustained)	20 Gpa	Silt	None
RCC Thermal Expansivity	10 x 10^{-6}/^{o}C	*Note:* *"Massless" foundation applied & Jt. 8 opening reduced by 0.72 mm on all analyses to compensate for gravitational modelling effects (see 5.3.2.5).*	
RCC Poisson's Ratio	0.2		
Foundation Elastic Modulus	15 GPa		
Foundation Poisson's Ratio	0.2		
Foundation Thermal Expansivity	10 x 10^{-6}/^{o}C		

* - The issue of the applied uplift pressure is discussed in **Appendix B**.

Finite Element Model

The same structural FE model described earlier in this Chapter was applied for the analyses undertaken, with a foundation rockmass extending 1.5 x the dam height upstream, downstream and beneath the dam and 1 x the dam height on either flank. The boundaries of the foundation model were fully constrained against movement.

As discussed earier, the common practice of adopting a massless foundation[9] for FE analysis requires that gravity is imposed as a load on the dam structure, but not on the foundation. This gives rise to a distortion of certain displacements, particularly close to the foundation where unrealistic shears are indicated on the model. An analysis indicated that the central opening on Joint No. 8 at RL 66.25 m was increased by 0.72 mm by this modelling effect. The openings on Joint Nos. 14 and 17 were not affected. Consequently, for comparison with measurements on the actual dam, 0.72 mm was deducted from the central opening indicated for Joint No. 8 on all analyses.

Materials Models / Loading Cases

With the above listed properties as constant, a net core temperature drop from placement of 8°C, as indicated on the installed instrumentation for winter 1993, was applied together with a number, or range of possible RCC creep/shrinkage behaviour scenarios, as indicated in **Table 5.7**. In accordance with the findings of the previous

analysis, a model that assumed an 8°C core temperature drop in conjunction with an 11°C external, or surface zone drop, as indicated in **Figure 5.12** (Scenario 2), was also investigated. Scenarios 1 and 2 accordingly represent the same situation of no autogenous/drying shrinkage and no creep of the RCC during the hydration and cooling cycle, with Scenario 2 simply representing a refinement based on the apparent differences in core and surface temperature drops that were found to be evident through a detailed examination of the recorded instrumentation data.

Table 5.7: Analysis Scenarios

Scenario	**Temperature Drop** (°C)		**Volume Reduction /Shrinkage** (microstrain)	**Effective Total Temperature Drop** (°C)
	Core	**Surface**		
1	8	8	0	8
2	8	11	0	8 / 11
3	8	8	70	15
4	8	8	160	25
5	8	8	300	38

Analysis Results

The following presents a summary of the displacement results obtained through the analyses completed. For the purposes of clarity of presentation, only the key results and findings are illustrated in this Chapter. A more comprehensive set of output and results, however, is included in **Appendix B** and that presentation describes in greater detail the impacts of the temperature drop, or shrinkage, on the structural function of the dam wall, with displacement plots and stress plots for each of the listed Scenarios.

The total horizontal displacements at the reference points and central joint openings at elevation RL 66.25 m predicted by the FE model for each of the Scenarios developed are listed in **Table 5.8**.

Table 5.8: Predicted Horizontal Displacements & Openings

Scenario	Effective Total Temp. Drop (°C)	Displacements (mm)						Central Joint Openings (mm)			
		P113	P120	P212	P217	P221	Total	Jt. 8	Jt.14	Jt.17	Total
1	8	12.7	8.4	8.8	10.1	6.1	46.1	1.17	0.77	1.56	3.50
2	8 / 11	14.3	8.6	9.4	12.4	6.8	51.5	1.20	0.46	1.88	3.54
3	15	18.1	10.0	11.7	14.4	7.7	61.9	4.60	2.67	4.54	11.81
4	25	26.1	13.2	15.1	17.3	10.9	82.6	10.16	5.58	8.51	24.25
5	38	35.3	16.5	20.3	21.3	13.6	107.0	10.83	9.75	13.60	34.18

Result Discussion

The above results can be compared with the equivalent figures measured on the prototype structure in July 1993, as listed in **Table 5.9** (and Table 5.5).

Table 5.9: Measured Displacements & Openings(2, 3, 4, 5 & Appendix B)

Measured Data	Displacements (mm)						Central Joint Openings (mm)			
	P113	P120	P212	P217	P221	Total	Jt. 8	Jt. 14	Jt. 17	Total
	14.5	11.7*	7.65	10.1	7.5*	51.5	1.00	0.95	1.45	3.40

The levels of confidence in the data indicated "*" are not considered as high.

Ignoring the displacement at P120, it is significant to note that the measured displacements and joint openings are generally less than any of those predicted applying the modelling scenarios considered. However, within a realistic level of accuracy, it is considered that the models applied under Scenarios 1 and 2 realistically represent the actual behaviour. Certainly, it can be stated that the crest displacements predicted for the "traditional" RCC materials model presented under Scenario 4 are almost double those measured on the prototype, while the predicted joint openings are sevenfold those actually measured.

Even a net 70 microstrain volume reduction (Scenario 3) as a result of shrinkage and stress relaxation creep would have given rise to a total joint opening of approximately 3.5 times that measured in reality.

It should be borne in mind that the analyses presented assume a fully linear concrete Deformation Modulus. Even though the value used is relatively high for a long-term modulus, in reality a non-linear stress-strain relationship will exist and the modulus that would in fact apply at the low levels of stress within the majority of the dam structure would result in reduced crest displacements. Experience with many structural dam analyses suggests that this impact might reduce the total crest displacements by 10 to 20% where no, or only minor heel tensions are evident. Conversely, experience of analysis using the COSMOS system would suggest that the crest displacements are likely to be over-estimated, by 5 to 15% compared to those predicted using other FE systems. In addition, where heel tensions are high, as is the case for Scenarios 3 to 5, it is quite possible that the elastic analyses under-state the actual displacements that would be developed. Accordingly, while it is clear that an absolute reproduction of the measured crest displacements will not be possible using a FE model, the crest displacements predicted using an elastic analysis with the COSMOS[8] FE system are probably as realistically comparable with those of the prototype structure as can be expected to be achieved.

Evaluating the crest displacements against those measured within the upper drainage gallery, a greater level of accuracy is considered to exist in respect of the predicted displacements for the latter location. Taking into account the larger than expected crest movements on the right flank, it is suggested that the full crest of the dam is probably subject to greater temperatures during summer than measured at the upper gallery level. This has almost certainly resulted in an inaccurate, but conservative, estimation of the “zero” displacement location for the crest monitoring points, which has consequently exaggerated the total downstream displacement considered to be the result of hydrostatic loading and temperature drop.

Considering the above factors and the findings of the temperature drop distribution analysis, it is postulated that Scenario 2 is probably most realistically representative of the actual RCC behaviour at Wolwedans Dam.

Sensitivity Analysis

In order to test the sensitivity of the above results, additional analyses were completed to review possible scenarios of increased RCC E modulus in conjunction with some creep/shrinkage. **Table 5.10** lists the associated characteristics, the loads evaluated, the predicted summed induced joint openings at RL 66.25 m and the downstream displacements at reference points P113 and P217, respectively.

Table 5.10: Sensitivity Analysis Results

Characteristics							Displacements		
Scenario	**Uplift**	**E Modulus Dam**	**E Modulus Foundation**	**Thermal Expansion Coefficient**	**Temperature Drop**	**Creep/ Shrikage**	Combined Induced Joint Opening	P113	P217
No.	% Design	(GPa)	(GPa)	(x 10^{-6}/°C)	(°C)	(Micro-strain)	(mm)	(mm)	(mm)
6	50	15	15	10	8	10	3.85	14.70	11.60
7	50	15	15	11	8	0	3.63	14.60	11.50
8	50	25	15	10	8	10	4.97	12.1	10.11
9	50	25	15	10	8	20	6.24	12.71	10.68
10	50	25	15	10	8	30	7.42	13.51	11.38

The analysis results presented in **Table 5.10** demonstrate that applying some creep/shrinkage for a lower RCC E modulus, it is possible to reproduce joint openings of the order measured on the prototype, but at the expense of higher crest and upper gallery-level displacements. Conversely, the measured crest and upper-gallery displacements can be reproduced with a higher RCC modulus and some creep, but only with higher induced joint openings. The analyses accordingly demonstrated that both the measured induced joint openings and the crest displacements could only realistically be reproduced with a no creep and 20 GPa RCC E modulus scenario.

Summary & Conclusions

The above analysis clearly demonstrates that Scenarios 1 and 2 most closely replicate the actual field measurements. Even the apparent surface creep effects caused by the temperature gradients across the section, as discussed earlier in this Chapter and as presented in Scenario 2, might seem to represent a conservative assumption.

The use of elastic materials properties for analysis may have resulted in marginally conservative displacement results, but the reference displacements are also conservative and the evident correlation accuracy between the crest displacements and the joint openings adds further confidence to the results presented and the validity of the assumed RCC materials behaviour. As demonstrated, a higher E modulus for the dam RCC in conjunction with some creep might be able to reproduce similar crest displacements to the prototype, but at the expense of significantly greater induced joint openings than were actually evident.

While the accuracy with which the application of a "no creep and no shrinkage" RCC materials model can reproduce the prototype behaviour is impressive, much more significant is the unquestionable invalidity of the traditional RCC materials model, as represented by Scenario 4. The significant increase in the crest displacements and

joint openings that result with even an additional 7 degrees of temperature drop (or 70 microstrain shrinkage) strongly suggest a “no creep and no shrinkage” situation for the RCC at Wolwedans Dam.

The anomalous behaviour in respect of the displacements read at P120, when compared to P113, and the generally excessive displacements apparent on the upper right flank of the dam demonstrates the complexity of analysis of the effects under scrutiny and confirms that it is simply not realistic, nor possible, to expect a completely accurate correlation between a FE model and a prototype dam.

The results of the analyses presented are not considered valid justification as a basis to conclude that the precise behaviour of the constituent RCC of Wolwedans Dam has been identified and that no creep and no shrinkage was accordingly evident. Such a conclusion was indeed never the objective of this study. There are too many variations of input parameters, too many variables in respect of non-linear materials behaviour and the foundation deformation characteristics to draw any precise conclusions.

Although an alternative scenario is not obvious, it cannot be concluded with certainty that extensive fine-tuning of the dam and foundation E moduli, the coefficient of thermal expansion, etc, etc, might not identify a solution that would include some creep in the RCC. However, it can be stated with absolute certainty that if such a scenario exists, the associated level of creep could not exceed a few tens of microstrain and certainly would be a great deal less than is applied in the conventional design approach for RCC dams.

The analysis presented can accordingly be considered to answer definitively one specific research question. Applying the typical CVC creep/shrinkage assumptions traditionally assumed in dam design is not valid in the case of high quality, high-paste RCC.

5.6. ANALYSIS 4: THERMAL ANALYSIS FOR CHANGUINOLA 1 DAM

5.6.1. BACKGROUND

At the time of writing, approximately one third of the volume of RCC required for the construction of the 105 m high Changuinola 1 Dam in Panama had been placed. While some of the main instrumentation had been installed, the available records were too short to be of any value. A strain gauge installed perpendicular to the dam axis in the first RCC placement, however, has provided some very interesting data over a period of seven months, confirming a very similar pattern of behaviour to the similarly installed instruments at Çine Dam.

Furthermore, a detailed Thermal study for the dam[17] has been completed and this analysis proved very effective in modelling the early RCC behaviour, accurately predicting the development of two surface gradient cracks. It is accordingly considered that worthwhile information from the Changuinola 1 Dam is available for inclusion in the investigations presented and accordingly, the indications of RCC behaviour that can be derived through correlating measurements, observations and analysis at this early stage are presented in this Chapter.

5.6.2. INTRODUCTION

A summarised description of the methodology applied for the Changuinola 1 Dam Thermal Analysis is provided in this Chapter and the findings of the study are compared with the behaviour observed to date. The Thermal Analysis included a sensitivity study, with the objective of developing a greater understanding of the behaviour of the placed RCC under the measured hydration temperature rise and this is subsequently addressed.

The general arrangements, the RCC mix and the instrumentation for Changuinola 1 Dam are presented in Chapter 2, while the data from the first strain gauge are presented and briefly discussed in Chapter 4.

The RCC placed at Chaguinola 1 Dam is a high-workability mix, with a modified Vebe time of 6 to 8 seconds. The high workability allows compaction with an immersion vibrator, without the addition of supplementary grout, although this technique is only used where the finish will not be exposed during operation and beneath the reinforced concrete of the chute spillway.

Plate 5.4: RCC Placement at Changuinola 1

5.6.3. CONSTRUCTION APPROACH

Before addressing the actual analysis undertaken, it is considered of value to describe the construction approach applied for Changuinola 1 Dam, as this was seen to be of specific influence on the levels of thermal stresses developed in the structure.

From approximately 40 m height, Changuinola 1 Dam will be constructed in a conventional manner, placing RCC continuously between abutments. Up to that level, however, in order to accommodate seasonal river flow and to maximise the RCC placement period, placement was split into two components. While excavation and foundation preparation was underway in the main river course, RCC placement was initiated around the river diversion culvert, comprising two 9 x 9 m culverts, on the right flank. On completion of consolidation grouting and the placement of dental concrete on the foundation in the original river course, the location of the RCC delivery system was re-routed and RCC placement was initiated on the left flank, as illustrated on **Plate 5.5**.

Plate 5.5: RCC Placement at Changuinola 1

This approach implied that the RCC surface on the right flank at elevation 111.375 mASL was left exposed for a period of approximately 10 weeks and a crack was observed approximately midway across the block, running parallel to the dam axis, at the end of the first week of June 2010.

5.6.4. MATERIALS COMPOSITION & PROPERTIES

5.6.4.1. General

The Changuinola 1 RCC contains 70 kg/m^3 of Portland cement, blended with 145 kg/m^3 of fly ash and testing on the full-scale trials revealed an adiabatic hydration temperature of the order of 21°C, which is high for an RCC and suggests that the cement used evolves a relatively high hydration heat energy.

Laboratory testing indicated the following RCC materials characteristics:

Table 5.11: Changuinola 1 RCC Laboratory Testing Results[18]

Property	Unit	Value
Coefficient of Thermal Expansion	Strain/°K	8.8 x 10^{-6}
Thermal Diffusivity	m^2/hr	0.002415
Compressive Strength (365 days)	MPa	36.2
Tensile Strength (56 days)	MPa	1.8
Density	KN/m^3	24.6
Poissons Ratio	-	0.2

The following properties were calculated on the basis of an empirical knowledge of the constituent materials:

Table 5.12: Changuinola 1 RCC – Calculated/Estimated Properties

Property	Unit	Value
Specific Heat Capacity	J/Kg.°K	980.9
Thermal Conductivity*	W/m.°K	1.65

* - For concrete, values of Thermal Conductivity usually lie between 2 and 4 W/m.°K and the value indicated for Changuinola 1 is accordingly unusually low. While this may well be a laboratory error, the associated implications are that the dissipation time for the hydration heat will be artificially extended.

5.6.4.2. Elastic Modulus

An age-dependent value for the RCC Elastic Modulus was applied for the Thermal Analysis, calculated on the basis of the tested compressive strength development. On the basis of the average compressive strength indicated on **Figure 5.23** the equivalent instantaneous E modulus value was calculated in accordance with the equation:

$$E_c = 57\,000 \sqrt{f'c}\ (\text{PSI})$$ [19 & 20]

where $f'c$ is the RCC cylinder strength = 0.78 f_{cu}

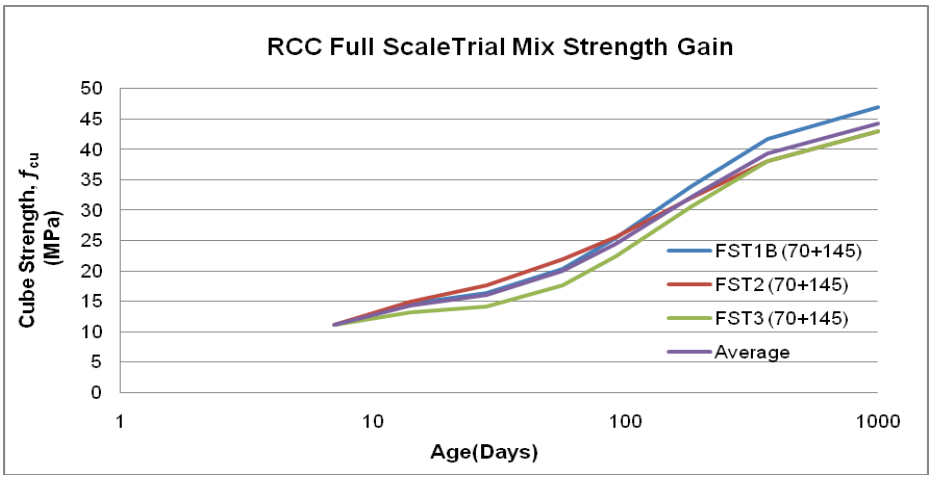

Figure 5.23: RCC Strength-Age Relationship[17]

The consequential values of instantaneous E modulus were reduced by 1/3 to represent sustained values and the derived age relationship for the E value applied for the Thermal Analysis is presented in **Figure 5.24**.

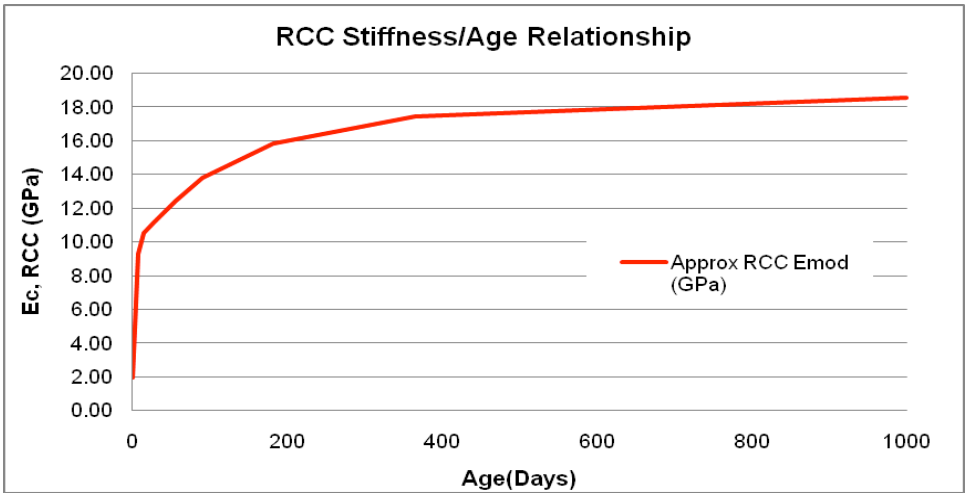

Figure 5.24: RCC E Modulus-Age Relationship[17]

For RCC ages beyond 2 years, a constant value of 18 GPa was assumed for the sustained E modulus.

5.6.4.3. Tensile Strength & Cracking

Computing tensile stresses on the basis of the time-dependent E modulus value, the tensile strength of the parent RCC was assumed to be equivalent to the 56 day value of 1.8 MPa indicated from testing on the full scale trials.

To evaluate the potential development of tensile cracking, the recommendations of the USACE's EP 1110-2-12 *Seismic Design Provisions for Roller Compacted Concrete Dams.* 1995[18] were applied as follows:

for $f_t < 0.6\ f_t'$, i.e. $f_t < 1.08$ MPa, No cracking is expected;

for $0.6\ f_{t'} < f_t < 1.25\ f_{t'}$, i.e. 1.08 MPa $< f_t <$ 2.25 MPa, Surface cracking is anticipated;

for $1.25\ f_{t'} < f_t < 1.33\ f_{t'}$, i.e. 2.25 MPa $< f_t <$ 2.4 MPa, Macro cracking is expected;

where $f_{t'}$ = Indicated tensile stress & f_t = Peak Tensile Strength (1.8 MPa).

The temeparture gradients and associated stresses for the analysis addressed were reviewed at 31st May, 30th June and 31st July, when the RCC at elevation 111.375 mASL on the right flank block had reached ages of 42, 72 and 103 days, respectively.

According to the testing from the full-scale trials, the 56 day age compressive strength of the RCC at Changuinola will be approximately 21 – 22 MPa, implying that the tensile strength is approximately 8.5% of the compressive strength.

Extrapolating from the RCC strength testing records for the full scale trials would suggest compressive strengths for the RCC at 42, 72 and 103 days age of approximately 19.2, 24.8 and 27.6 MPa, respectively.

Applying a similar tensile/compressive strength ratio as indicated for the 56 day test results would suggest tensile strengths at 42 days age of 1.6 MPa, 72 days age of 2.1 MPa and 103 days age of 2.35 MPa, respectively. On the basis of the anticipated crack development criteria above, it would accordingly be anticipated that cracking would become visible on the surface at elevation 111.375 mASL for tensile stresses exceeding approximately 2 MPa by 31st May, 2.6 MPa by 30th June and/or 2.9 MPa by 31st July, respectively.

5.6.5. THERMAL ANALYSIS

5.6.5.1. Analysis Objectives

The objectives of the Thermal Analysis for Changuinola 1 Dam can be defined as follows:

- To confirm the appropriateness of the maximum allowable RCC placement temperature of 29°C.
- To investigate the impact of the phase construction approach.
- To confirm the appropriateness of the proposed 20 m induced joint spacing.

To achieve the above objectives, the analysis was structured on the following basis:

1. Develop the anticipated temperature histories during construction.
2. Develop the long-term temperature histories until the trapped hydration heat is fully dissipated and thereby predict long-term stable seasonal temperature distributions.
3. Analyse the initial temperature histories for associated stress and consequential surface gradient cracking.
4. Analyse long-term temperature histories for associated stress (with and without creep) and consequential mass gradient cracking.
5. Predict contraction joint openings.

It is not intended to address the full analysis in the study presented herein, but rather to focus on the related findings and implications of the Thermal Analysis in respect to the early behaviour of the constituent RCC.

5.6.5.2. Analysis Approach

General

A comprehensive transient thermal analysis was completed for Changuinola 1 Dam, modelling the actual construction sequence applied for the first one third of the RCC placed and the intended programme for the balance. On the spillway section, the analysis also included the construction of the reinforced concrete chute, placed on top of the RCC, but lagging RCC placement by a period of not less than 2 weeks.

The transient thermal analysis was used to determine the evolution of the temperature distributions across two critical sections at a number of intervals from 1 week to 40 years, while the same distributions were subsequently analysed for associated strain and stress distributions and these were evaluated for the potential development of cracks.

Modelling

The Finite Element Mesh for the analysis was constructed in 300 mm layers, as applied in reality on the dam, with 300 x 300 mm elements. Weekly construction progress was modelled using a daily time step, with the evolution of the full hydration heat assumed over 7 days. The hydration temperature development, as per **Figure 5.25**, was converted into an associated daily heat energy value (W/m^2) and this was applied to each element within the mesh individually. In this manner, the hydration heat evolution was allowed to develop concurrently with convection and radiation dissipation at the exposed surfaces, simulating the actual situation in which core temperature rises due to hydration are significantly greater than surface values.

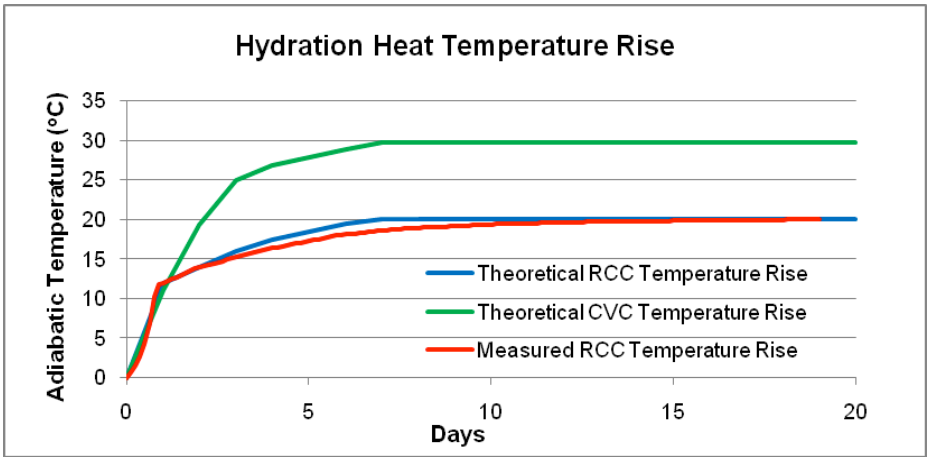

Figure 5.25: Concrete Hydration Temperature Development[16]

For the Thermal Analysis, the COSMOS[8] GeoStar and DesignStar Finite Element software was used, applying 2-dimensional shell element for the sectional analyses and 3-dimensional tetrahedral solid elements for the long-term evaluation of the induced joint spacings and predictions of associated openings.

Simulating RCC placement temperatures on the basis of average monthly temperatures increased by 2°C to allow for mixing and handling heat inputs, the surfaces of the structure, as placed in weekly intervals, were exposed to the external climatic conditions using surface convection on the basis of a nominally assumed wind speed. In addition, assumed values of solar radiation were applied and an estimated heat transfer coefficient was applied for the gallery surfaces, together with estimated gallery air temperature variations. After March 2011, an increased heat transfer coefficient was applied to the upstream face, in conjunction with appropriate seasonal water temperature variations with depth to simulate the presence of the dam reservoir.

The modes of heat development and dissipation applied for analysis during construction and long-term operation are illustrated in a simplified format in **Figures 5.26** and **5.27**.

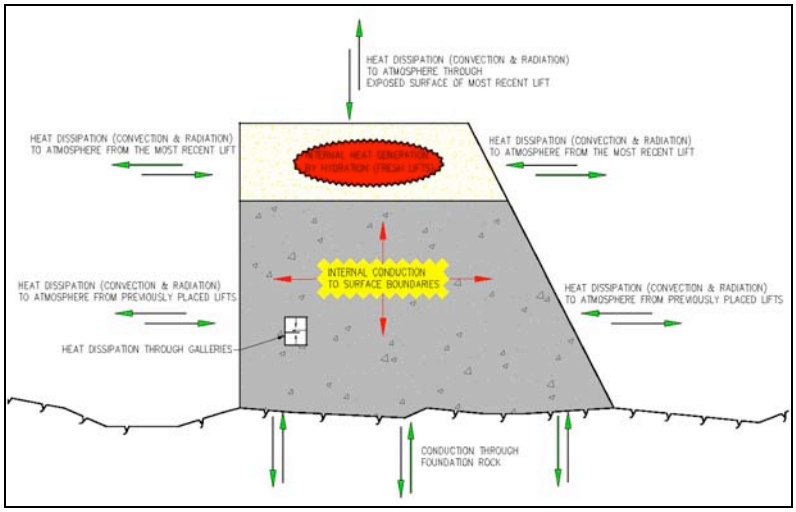

Figure 5.26: Thermal Model Heat Inputs & Losses During Construction[16]

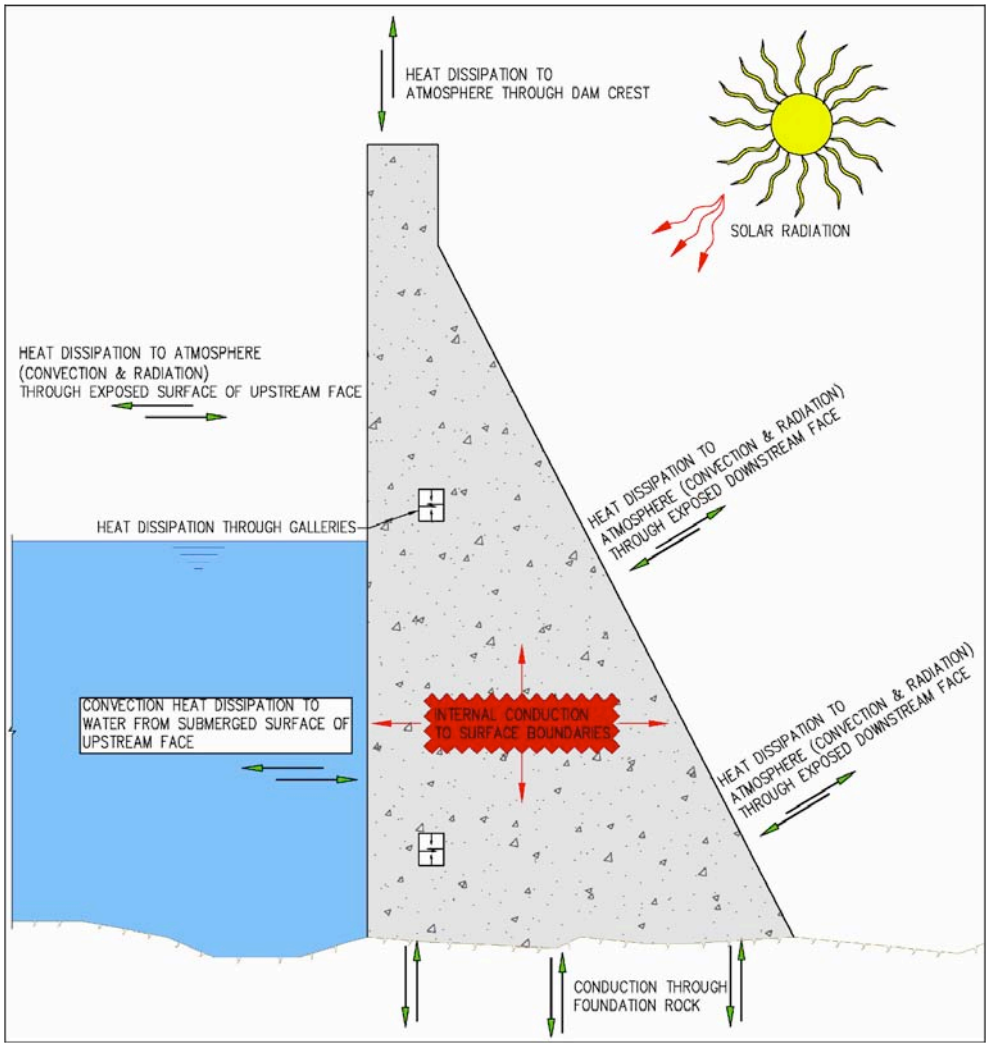

Figure 5.27: Long-Term Thermal Model Heat Inputs & Losses(16)

Relevant Analyses

For the purposes of this Thesis, only the analysis that can be compared with measured behaviour and observations to date is addressed and this accordingly deals with the first placement to elevation 111.375 m on the right flank (as illustrated on **Plate 5.5**).

The analysis addressed accordingly deals with the placement of RCC in the right side block from foundation level to elevations 111.375 mASL, which was undertaken between the beginning of December 2009 and 20th April 2010, with a break between 1st January and 2nd March while the RCC placement in this area was stopped at elevation 90.975 mASL. After exposure for a period of approximately 7 weeks, a crack was noticed in the surface at elevation 111.375 mASL and the primary objective of the analysis addressed is to provide an interpretation of this observation, considering the measured behaviour of this RCC, as indicated on the installed strain gauge.

For this evaluation, two scenarios of RCC behaviour were considered:

- **Scenario 1** assumes no creep in the core RCC.
- **Scenario 2** assumes creep of the order of 25 microns in the core RCC.

As mentioned elsewhere in this Thesis, the occurrence of creep as a consequence of internal restraint within the core of mass concrete is often considered as advantageous from the point of view of reducing the occurrence of surface cracking due to excessive thermal gradients. Correspondingly, an assumption of no creep in this situation would be considered conservative in enabling a review of the maximum possible surface tensile stresses that could develop as a result of temperature gradients.

Scenario 2 includes the effect of approximately 25 microns of creep by reducing the maximum core RCC temperature by 3°C, effectively limiting the total core thermal expansion as a result by 8.8 x 10^{-6} x 3°C = 26.4 microstrain.

5.6.5.3. Analysis Results

General

While extracts from the preliminary thermal analysis dealing with the joint spacing design and the arch design for Changuinola 1 Dam are presented in Chapter 7, only the results of the detailed thermal analysis relating to the surface gradient cracking evaluation of the first placement to elevation 111.375 m on the right flank are addressed in this Chapter.

Presentation of Results

The results of the surface gradient analysis undertaken are presented in **Figure 5.28** to **5.33** in the form of temperature and horizontal (upstream-downstream) stress distribution plots for the two creep scenarios at 31st May, 30th June and 31st July.

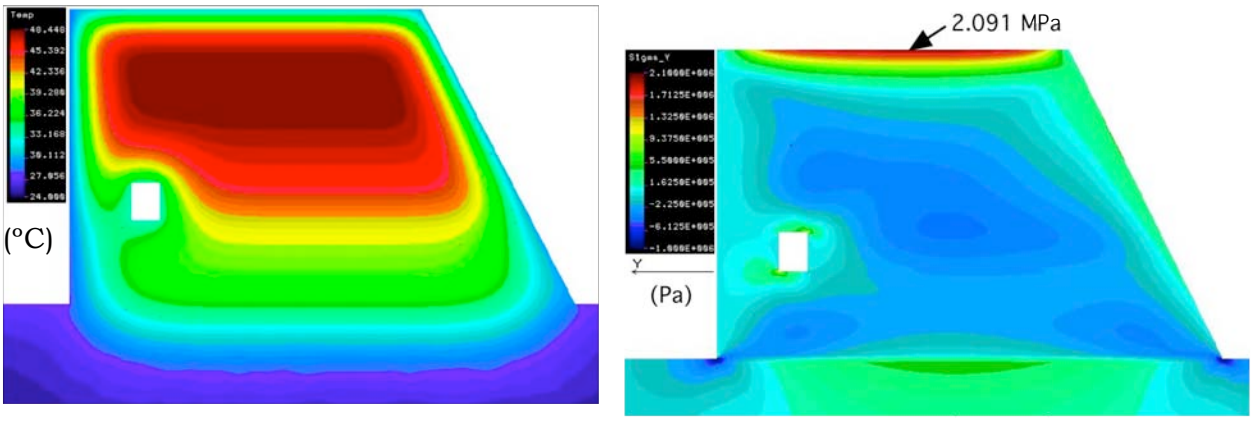

Figure 5.28: Temperature & Horizontal Stress Distributions 31 May 2010 – Scenario 1(17)

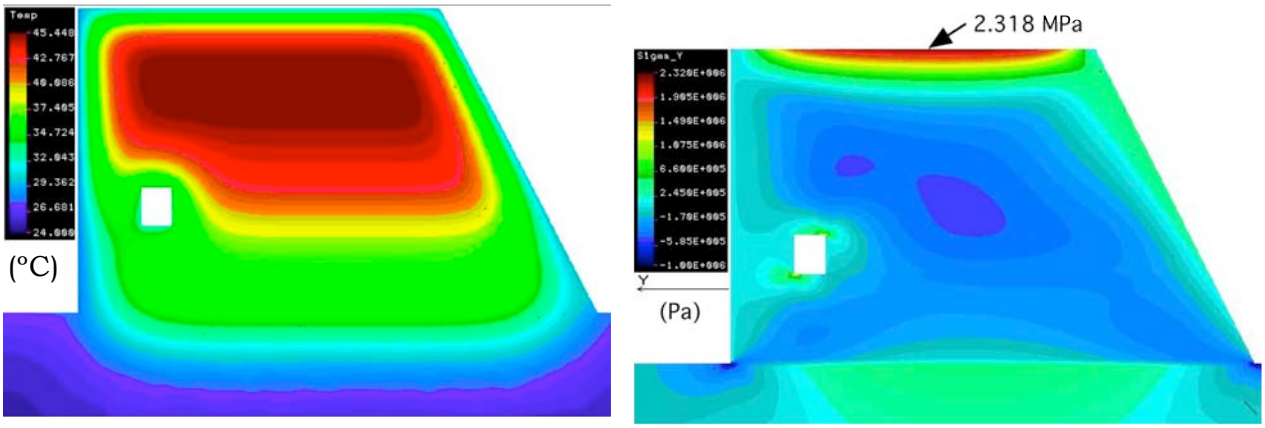

Figure 5.29: Temperature & Horizontal Stress Distributions 30 June 2010 – Scenario 1(17)

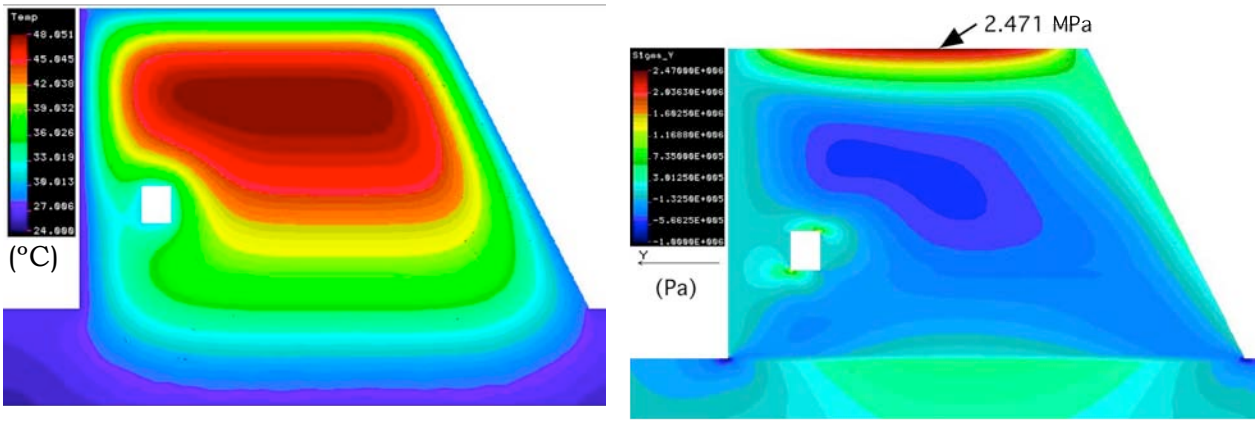

Figure 5.30: Temperature & Horizontal Stress Distributions 31 July 2010 – Scenario 1(17)

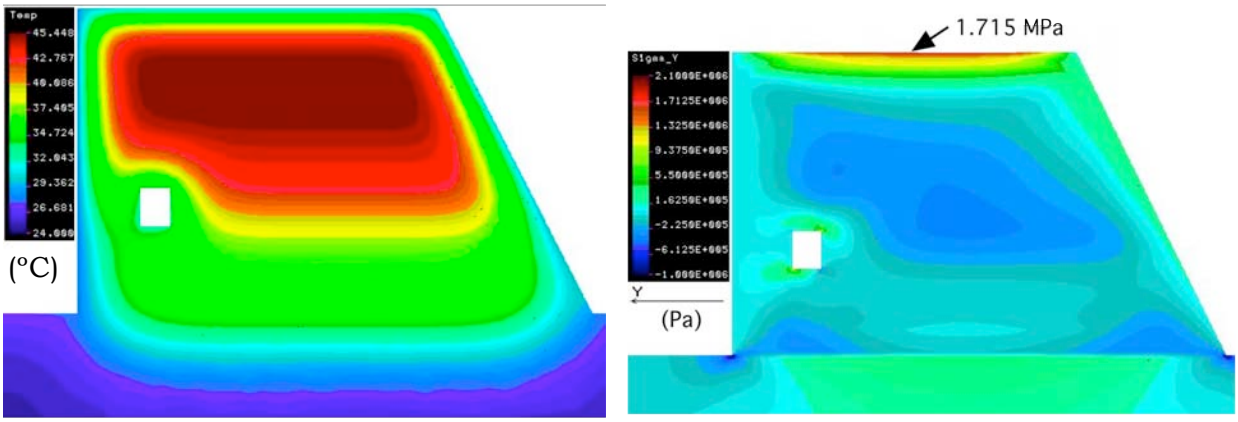

Figure 5.31: Temperature & Horizontal Stress Distributions 31 May 2010 – Scenario 2(17)

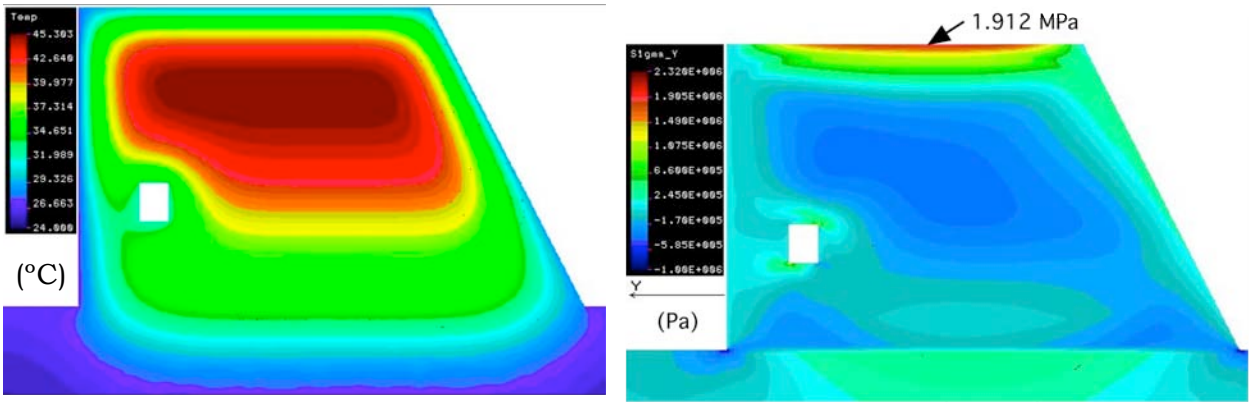

Figure 5.32: Temperature & Horizontal Stress Distributions 30 June 2010 – Scenario 2(17)

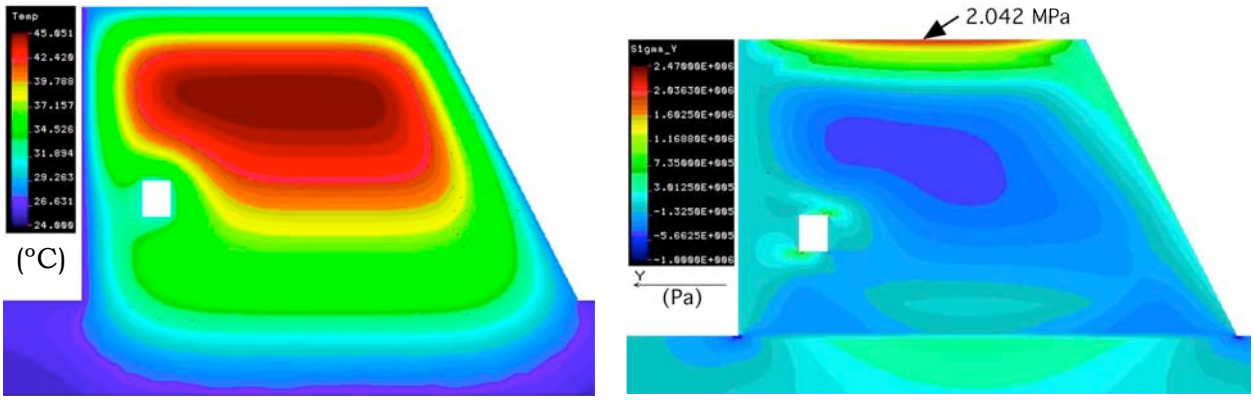

Figure 5.33: Temperature & Horizontal Stress Distributions 31 July 2010 – Scenario 2(17)

A summary of the critical maximum surface stresses indicated in the analysis is provide in **Table 5.13**.

Table 5.13: Summary of Tensile Stress Results

Scenario	**Maximum Surface Tensile Stress** (MPa)		
	31 May	30 June	31 July
Scenario 1	2.09	2.32	2.47
Scenario 2	1.72	1.91	2.04

Evaluating the above stresses in relation to the criteria established under 5.6.4.3, cracking could be anticipated under Scenario 1 by the end of May, while no cracking would be anticipated by the end of July for Scenario 2.

5.6.5.4. Conclusions

While the data from the strain gauge installed in the first RCC placement at Changuinola 1 Dam indicated unrestrained thermal expansion within the core, with no apparent reduction in expansion, or creep occurring as a consequence of internal restraint, the same effect is confirmed through the stress interpretation of the thermal analysis. The “no creep” Scenario 1 seems to closely replicate the observations made on the dam, while the introduction of just 25 microstrain of creep would appear to have been adequate to have prevented the evident crack from developing.

5.7. DISCUSSION

The analyses presented in this Chapter are considered to have produced some very interesting results. Certainly, it may not be realistic to conclude that high-paste RCC does not suffer from any shrinkage and creep, but this is a result of the typical level of accuracy with which the behaviour of a prototype dam can be analysed and the apparent unlikeliness of such a conclusion, rather than as a consequence of an inadequate strength of results. All of the analyses completed suggest the same pattern of behaviour for high quality, high-paste RCC in exhibiting negligible creep and/or shrinkage during the hydration heating and cooling cycle.

5.8. CONCLUSIONS

Although it may not be possible to simulate all of the actual displacements and joint openings measured with complete accuracy, the very significant difference between the displacements and joint openings measured compared with those that would have been anticipated if any significant creep and drying shrinkage had occurred leaves no ambiguity in the conclusions that must be drawn.

The analyses presented in this Chapter serve to confirm that the level of creep and shrinkage conventionally assumed for RCC, as discussed in Chapter 3, did not occur at Wolwedans Dam. This is consequently considered to answer one of the specific research questions posed and to correspondingly confirm that adopting the same design approach as has been traditionally applied for CVC in respect of the concrete volume reduction experienced during the hydration heating and cooling cycle is not necessarily valid for high-paste RCC.

5.9. A NEW UNDERSTANDING OF THE EARLY BEHAVIOUR OF RCC IN LARGE DAMS

5.9.1. DISCUSSING THE IMPACT OF A NEW UNDERSTANDING OF EARLY RCC BEHAVIOUR

On the basis of the analyses completed, it is would seem that a new design approach for joint spacings in RCC dams can, and should, be developed. The findings presented can readily be applied to establish the levels of residual stress within the body of an RCC dam wall for specific, selected induced joint spacings, thereby allowing the design of appropriate joint spacings.

The findings presented in this Chapter are considered of particular importance in relation to the design of RCC arch dams. While the findings suggest that lower temperature drop loadings than originally considered are in fact applicable, this can

present greater problems in respect to the grouting of induced joints on an RCC arch. If little, or no creep occurs during hydration heat development and dissipation, post-cooling of RCC performs no function other than limiting differential temperatures and potentially lowering the RCC temperature to facilitate joint grouting. Such an eventuality, however, also implies that a greater lowering of temperature is necessary before joint opening is initiated and any grouting becomes possible.

The analyses addressed are furthermore of particular relevance in respect of the susceptibility of large RCC dam structures to cracking parallel to the axis. In view of the fact that such cracking will occur as a consequence of long term temperature drop loads within the well insulated internal core zones of a dam wall, it is considered that the principle findings have an immediate and direct application in respect of this condition.

5.9.2. FURTHER DEVELOPING THE UNDERSTANDING OF EARLY RCC BEHAVIOUR

On the basis of the investigations and analyses completed, it is considered appropriate to attempt to develop an understanding of the reasons that RCC is apparently less susceptible to early shrinkage and creep than is the case for CVC. In Chapter 6, these issues are discussed and a new understanding of the early behaviour of RCC is proposed.

5.10. REFERENCES

[1] Shaw QHW, Geringer JJ & Hollingworth F. *Mossel Bay (Wolwedans Dam) Government Water Scheme. Wolwedans Dam Completion Report*. DWAF Report No. K200/02/DE01. April 1993.

[2] Shaw QHW. *An Investigation into the Thermal Behaviour of RCC in Large Dams.* Proceedings. 5th International Symposium on Roller Compacted Concrete Dams. Guiyang, China. 2007

[3] Oosthuizen C. *Behaviour of Roller Compacted Concrete in Arch/Gravity Dams.* Proceedings. International Workshop on Dam Safety Evaluation. Grindelwald, Switzerland. April 1993.

[4] Oosthuizen C. *The Use of Field Instrumentation as an Aid to Determine the Behaviour of Roller Compacted Concrete in an Arch/Gravity Dam.* Proceedings. 3rd International Symposium on Field Instruments in Geomechanics. Oslo, Norway. September 1991.

[5] Oosthuizen C. *Performance of Roller Compacted Concrete in Arch/Gravity Dams.* Proceedings. 2nd International Symposium on Roller Compacted Concrete Dams. Santander, Spain. 1995.

[6] Hattingh LC, Heinz WF & Oosthuizen C. *Joint Grouting of a RCC Arch/Gravity Dam: Practical Aspects.* Proceedings. 2nd International Symposium on Roller Compacted Concrete Dams. Santander, Spain. pp 1037–1051. 1995.

[7] Precise Engineering Surveys. Department of Water Affairs. *Instrumentation Data for Wolwedans Dam. 1990 to 2008.* August 2008.

[8] Structural Research and Analysis Corporation (SRAC). *COSMOSM Finite Element Analysis Program.* General-purpose, modular FE Analysis system. SRAC, a division of SolidWorks Corporation, Dassault Systemes S.A., Paris, France.

[9] United States Army Corps of Engineers. *Time History Dynamic Analysis of Concrete Hydraulic Structures.* Engineering Manual, EM 1110-2-6051. USACE. Washington. December 2003.

[10] Owens, G. *Fulton's Concrete Technology.* Chapter 8. Ninth Edition. Cement & Concrete Institute. Midrand. RSA. 2009.

[11] United States Army Corps of Engineers. *Arch Dam Design.* Engineering Manual, EM 1110-2-2201. USACE. Washington. May 2004.

[12] United States Army Corps of Engineers. *Thermal Studies of Mass Concrete Structures.* Engineering Technical Letter, ETL 1110-2-542. USACE. Washington. May 1997.

[13] Shaw QHW. *The Role of Temperature in Relation to the Structural Behaviour of Continuously Constructed Roller Compacted Concrete and Rubble Masonry Concrete Arch Dams.* MSc Thesis, University of Brighton. UK. 2001.

[14] Hattingh LC. *Completion Report for the Crack Joint Grouting. Wolwednas Dam.* Mossel Bay Government water Scheme. Internal Department of Water Affairs & Forestry. Report No. K200-02-DD05. November 1994.

[15] Hattingh LC, Heinz WF & Oosthuizen C. *Joint Grouting of a RCC Arch/Gravity Dam: Practical Aspects.* 2nd International Symposium on Roller Compacted Concrete Dams. Santander, Spain. pp 1037-1051. 1995.

[16] Cai Q, Kotsiovos M & Durieux JH. *3-D Structural Analysis of Wolwedans Dam.* Internal Report No. K200/02/DK03. Sub-Directorate Structural Studies. Directorate Design Services. Department of Water Affairs & Forestry. Pretoria. February 1997.

[17] Greyling, RG & Shaw QHW. *Changuinola 1 Dam. Thermal Analysis Report.* Report No. 4178/11436-R1. MD&A. July 2010.

[18] Dunstan, MRH. *Changuinola 1 Dam. Review of the In-situ Properties of Full-Scale Trial 1B.* Report No. Chan1/461/090923. MD&A. September 2009.

[19] Neville, AM. *Properties of Concrete.* Chapter 9. Fourth Edition. Pearson Prentice Hall. London. 2002.

[20] United States Army Corps of Engineers. *Seismic Design Provisions for Roller Compacted Concrete Dams.* Engineering Pamphlet, EP 1110-2-12. USACE. Washington. September 1995.